Available online at www.sciencedirect.com
SCIENCE DIRECT®
ELSEVIER
Geomorphology 50 (2003) 83–110
GEOMORPHOLOGY
www.elsevier.com/locate/geomorph

Tectonically driven landscape development within the eastern Alpujarran Corridor, Betic Cordillera, SE Spain (Almería)

A.F. García [a,b,*], Z. Zhu [c,d], T.L. Ku [d], C. Sanz de Galdeano [e], O.A. Chadwick [a,f], J. Chacón Montero [b,g]

[a] *Department of Geological Sciences, The University of California, Santa Barbara, CA, USA*
[b] *Grupo de Investigaciones Medio Ambientales: Riesgos Naturales e Ingenieria del Terreno, University of Granada, Granada, Spain*
[c] *Guangzhou Institute of Geochemistry, Chinese Academy of Sciences, People's Republic of China*
[d] *Department of Earth Sciences, The University of Southern California, Los Angeles, CA 90089-0740, USA*
[e] *Instituto Andaluz de Ciencias de la Tierra, CSIC, Facultad de Ciencias, Universidad de Granada, C/ Severo Ochoa s/n, 18071 Granada, Spain*
[f] *Department of Geography, The University of California, Santa Barbara, CA 93106, USA*
[g] *Departamento de Ingeniería Civil, Universidad de Granada, C/ Severo Ochoa s/n, 18071 Granada, Spain*

Received 1 August 2000; received in revised form 1 May 2002; accepted 15 July 2002

Abstract

The Betic Cordillera is a topographic manifestation of Miocene to recent collision between the African and the European plates. Mountain ranges in the Internal Zone of the Betic Cordillera are exhumed massifs of metamorphic and sedimentary rocks, and are surrounded by low-lying sedimentary basins. The Neogene history of mountain range uplift and basin formation in the Betics is well studied, but Quaternary topographic development and its relation to convergent plate boundary tectonics is less understood. Deformation, rates of stream incision and factors controlling landscape evolution on the flanks of the highest mountains in the Betic Cordillera are studied to gain insight on the relationship of Quaternary tectonics to topographic development. Specifically, geomorphic processes that led to formation of topographic relief within the Internal Zone of the Betic Cordillera are assessed.

This paper is based on a field study conducted in the eastern Alpujarran Corridor (EAC), which is the eastern half of a 4–6 km wide and 80-km long inverted sedimentary basin. The Mid to Late Quaternary history of basin denudation is deduced on the basis of morphostratigraphic, geochronologic and structural–geologic analyses of oxygen isotope Stage 8-time fluvial deposits in the EAC.

Results of these analyses indicate that climate and faulting played only a minor role in landscape evolution in the EAC. Instead, the EAC topographic trough was excavated by a drainage network whose axial stream (Río Andarax) was incising at a rate between 0.3 and 0.7 m/ka since oxygen isotope Stage 8. This paper demonstrates that these incision rates are the same as regional rock uplift rates in the EAC. During the Mid and Late Quaternary, topographic relief between the EAC and adjacent mountain ranges developed largely as a result of fluvial denudation driven by regional uplift.

The implications of the results of this investigation are used to propose a model of Quaternary topographic relief development in the Internal Zone of Betic Cordillera. Topographic relief between Internal Zone bedrock massifs and adjacent

* Corresponding author. Present address: Physics Department, California Polytechnic State University, San Luis Obispo, CA 93407, USA.
E-mail address: afgarcia@calpoly.edu (A.F. García).

PII: S0169-555X(02)00209-X

basins formed largely as a result of fluvial denudation driven by regional uplift. Faulting also played a significant role in areas that are within a few kilometers of crustal-scale fault zones.

Keywords: Betic Cordillera; Quaternary; Sierra Nevada; Tectonics; Uplift

1. Introduction

The tectonically active Betic Cordillera of southern Spain is a major NE–SW trending topographic high consisting of E–W and NE–SW trending mountain ranges separated by lower lying sedimentary basins (Fig. 1). The altitude of Betic mountain range summits is typically between 1500 and 2500 m, and the altitude of the highest peaks is greater than 3000 m. The altitude of Betic basins ranges from near sea level at the coast to between 200 and 1000 m farther inland (Fig. 1).

The Betic Cordillera is a topographic manifestation of the collision between the African and European plates (Fig. 1). The Betic Cordillera began forming in the Late Miocene, and mountain building continues to recent times (e.g., Sanz de Galdeano and Vera, 1992). Although the history of mountain range uplift and basin formation from the Mid to Late Miocene through the Pliocene is well documented (e.g., Sanz de Galdeano and Vera, 1992), the Quaternary recent topographic development of the Betic Cordillera has received little attention.

Within the Betic Cordillera, the Alpujarran Corridor is in a notable topographic position because it is 10–15 km south of and parallel to the mountainous crest of Sierra Nevada, which is the highest topographic ridge in Betic Cordillera (Fig. 1). A 40-km long segment of the Sierra Nevada crest exceeds an altitude of 2000 m, and its highest peak (Mulhacén) is 3479 m above sea level. The structural location of the Alpujarran Corridor is interesting in an along-orogenic strike sense because it is between two areas where Late Miocene to recent African–European plate convergence is accommodated by different deformational styles. East of the Alpujarran Corridor, Late Miocene to present deformation is dominated by a crustal scale, left lateral shear zone that extends from Cabo de Gata to Alicante (Fig. 1; e.g., De Larouzière et al., 1988). This area has also been affected by Quaternary regional uplift (Mather, 2000). West of the Alpujarran Corridor, the Granada and Padul basins comprise an area where Late Miocene to present regional uplift and extensional tectonism predominate. The extensional tectonism includes at least 3 km of normal stratigraphic separation along border faults of basins (Fig. 1; e.g., Sanz de Galdeano and López Garrido, 1999).

This paper is based on results of the first detailed field study of the Quaternary geology and geomorphology of the eastern part of the Alpujarran Corridor (EAC). The purposes of this paper are to: (1) characterize the timing and style of Quaternary deformation in the EAC; (2) determine rates of fluvial incision in the EAC and use those rates to estimate rates of Late Quaternary regional uplift; (3) assess the factors that controlled Quaternary landscape development within the EAC; and (4) propose a conceptual model for generation of topographic relief within the Internal Zone of the Betic Cordillera during the Quaternary Period.

2. Regional tectonic and topographic development

The Betic Internal Zone nappe sequence formed east of its present location, and was displaced to the west during the Miocene (Sanz de Galdeano, 1990).

Fig. 1. Regional maps of western Europe and southern Spain. (a) Approximate location of the Betic Cordillera on a political map of western Europe and north Africa. (b) Simplified geologic map of the Betic Cordillera. The area referred to in the text as "the Betic Internal Zone" includes mountain ranges formed by uplifted Internal Zone rocks and adjacent Neogene/Quaternary basins. Names of basins discussed in the text are written in all capital letters. The "Betic Foreland" is shown geographically rather than in terms of rock type. (c) Topographic map of the central part of the Betic Internal Zone. Contour lines are altitude in meters.

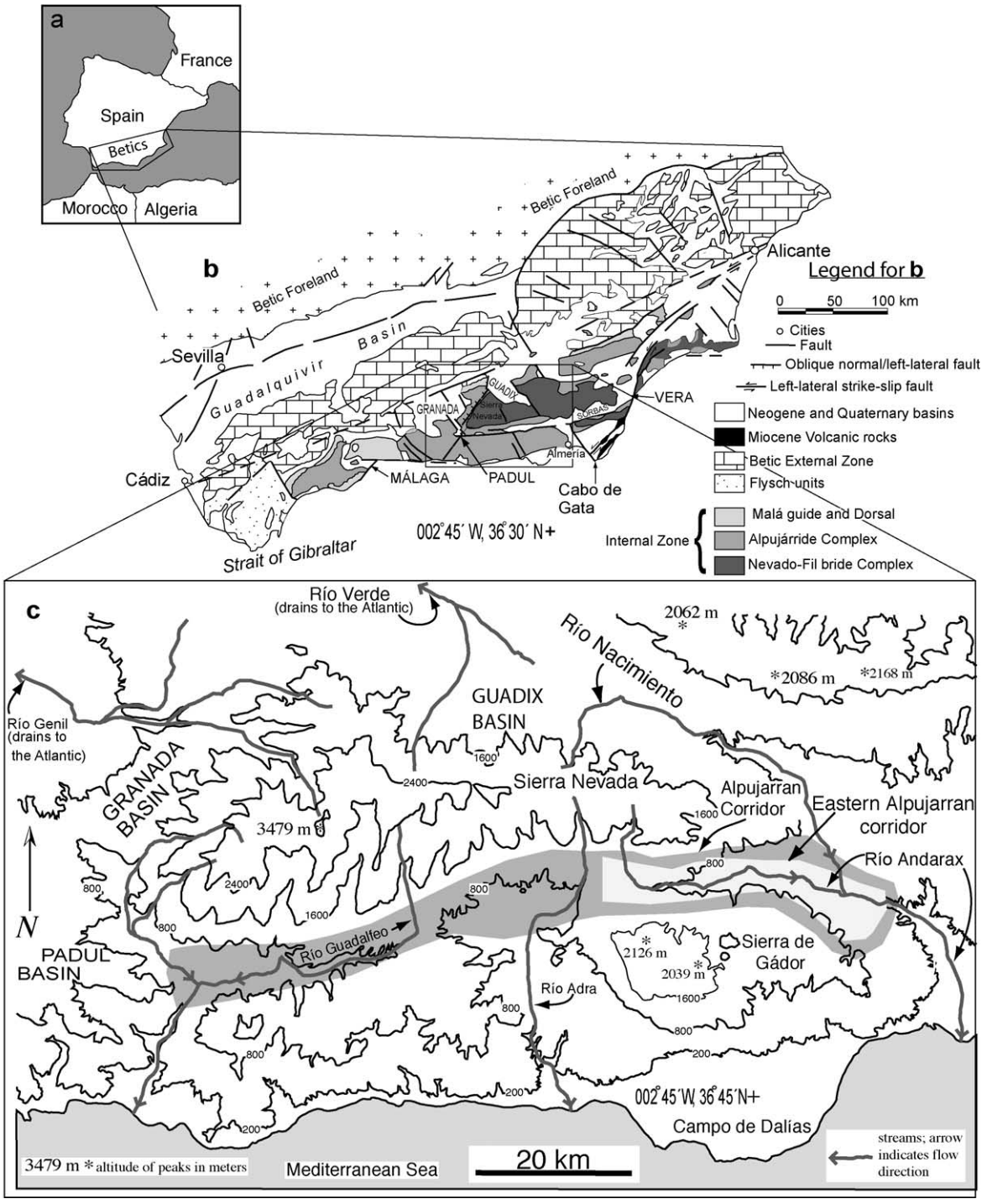
a
France
Spain
Betics
Morocco
Algeria
b
Betic Foreland
Betic Foreland
Alicante
Sevilla
Guadalquivir Basin
GUADIX
GRANADA
Sierra Nevada
VERA
Sierra de Gádor
Almería
Cádiz
MÁLAGA
PADUL
Cabo de Gata
002°45′ W, 36°30′ N+
Strait of Gibraltar
Legend for b
0 50 100 km
Cities
Fault
Oblique normal/left-lateral fault
Left-lateral strike-slip fault
Neogene and Quaternary basins
Miocene Volcanic rocks
Betic External Zone
Flysch-units
Internal Zone
Malá guide and Dorsal
Alpujárride Complex
Nevado-Fil bride Complex
c
Río Verde
(drains to the Atlantic)
Río Nacimiento
2062 m
*2086 m
*2168 m
Río Genil
(drains to
the Atlantic)
GUADIX
BASIN
GRANADA
BASIN
Sierra Nevada
Alpujarran
Corridor
Eastern Alpujarran
corridor
Río Andarax
3479 m
N
PADUL
BASIN
Río Guadalfeo
Río Adra
2126 m
2039 m
Sierra de
Gádor
002°45′W, 36°45′N+
Campo de Dalías
3479 m * altitude of peaks in meters
Mediterranean Sea
20 km
streams; arrow
indicates flow
direction

The Internal Zone was sutured to the Iberian Peninsula in Mid to Late Miocene time, and since then stress and strain in the Internal Zone have been dominated by N–S to NNW–SSE compression and shortening arising from African plate–European plate convergence (e.g., Sanz de Galdeano, 1990). Convergence led to underthrusting of the Iberian massif below the Internal Zone terrane, which in turn caused regional uplift of much of the Betic Cordillera Internal Zone through the Quaternary (Galindo-Zaldívar et al., 1997). Mid to Late Miocene through recent shortening in the upper and middle crust of the Internal Zone has been mostly accommodated by the formation of crustal-scale fault zones and E–W trending antiforms whose wavelengths and amplitudes are several tens of kilometers (e.g., Galindo-Zaldívar et al., 1997). Notable crustal-scale structures that were active in the Quaternary are a left lateral shear zone that extends from Cabo de Gata to Alicante (Fig. 1; De Larouzière et al., 1988) and an oblique normal/left lateral fault or fault zone in the Granada area (Fig. 1; Sanz de Galdeano and López Garrido, 1999).

The ca. 10-km wavelength antiforms comprise uplifted Internal Zone bedrock massifs that are organized in a series of E–W to NE–SW trending mountain ranges. They form the topographic highs in the Betic Cordillera. The topographic lows of the Betic Cordillera are sedimentary basins that in most cases were marine depocenters from the Late Miocene through the Late Pliocene (Fig. 1; Sanz de Galdeano and Vera, 1992). Most Neogene marine basins throughout the Internal Zone of the Betic Cordillera, including the EAC, were emergent by the Late Pliocene Epoch (Sanz de Galdeano and Vera, 1992). Emergence was related to epeirogenic uplift affecting the Internal Zone, and regional uplift continues through recent times (e.g., Galindo-Zaldívar et al., 1997; Mather, 2000).

The Alpujarran Corridor is one of several E–W trending structural corridors in the Betic Cordillera (Sanz de Galdeano, 1996). Most of the faults that define the Alpujarran Corridor formed during the Miocene time, westward displacement of the Internal Zone terrane relative to the Iberian craton (Sanz de Galdeano, 1996). The dominant structures of the Alpujarran Corridor are two 80-km long fault zones that are between 2 and 6 km apart and that have accommodated between 40 and 75 km of right lateral strike-slip separation and up to 2 km of vertical separation (Fig. 2; Sanz de Galdeano, 1996). Faults within these zones are typically 10 km long, strike 90° to 70° and are mostly high angle to vertical (Sanz de Galdeano, 1996) (Fig. 2).

3. Pre-Quaternary geology of the EAC

Rock type is a fundamental control on landscape evolution. Therefore, deducing factors that control landscape evolution requires understanding bedrock geometry and structure. The pre-Quaternary rock types within the EAC, and their distribution, are characterized in this section.

3.1. Metamorphic basement

Rocks exposed in mountain ranges adjacent to the Alpujarran Corridor, and the rocks that the Alpujarran structural basin is formed in, are part of the Betic Internal Zone nappe sequence (Sanz de Galdeano, 1997) (Fig. 1). Adjacent to the Alpujarran Corridor, the Sierra Nevada is underlain largely by pelitic, high-grade metamorphic rocks of the Nevado–Filábride Complex nappe (Figs. 1 and 2). An E–W trending band of the Alpujárride Complex nappe rocks, which is up to 1 km wide, is present along the southern flank of Sierra Nevada (Fig. 2). The Sierra de Gádor is almost entirely underlain by marble and dolomite of the Alpujárride Complex (Ta; Figs. 2–4). Near the town of Alhama de Almería, the Sierra de Gádor mountain front is locally formed in thrust sheets of the Felix Unit of the Alpujárride Complex (IGME, 1980). The Felix Unit in the Sierra de Gádor is mostly lavender and bright blue phyllite and calcschist (Sanz de Galdeano, 1997).

3.2. Miocene basin-fill sediments

Miocene basin-fill sediments (Mcs; Figs. 3 and 4) are typically in fault contact with Alpujárride Complex rocks along vertical and subvertical faults (Sanz de Galdeano, 1996; Figs. 3–5). These Miocene sediments are unconsolidated Middle Miocene marls, as well as unconsolidated Late Miocene interbedded marls, sands and gravels (Sanz de Galdeano et al.,

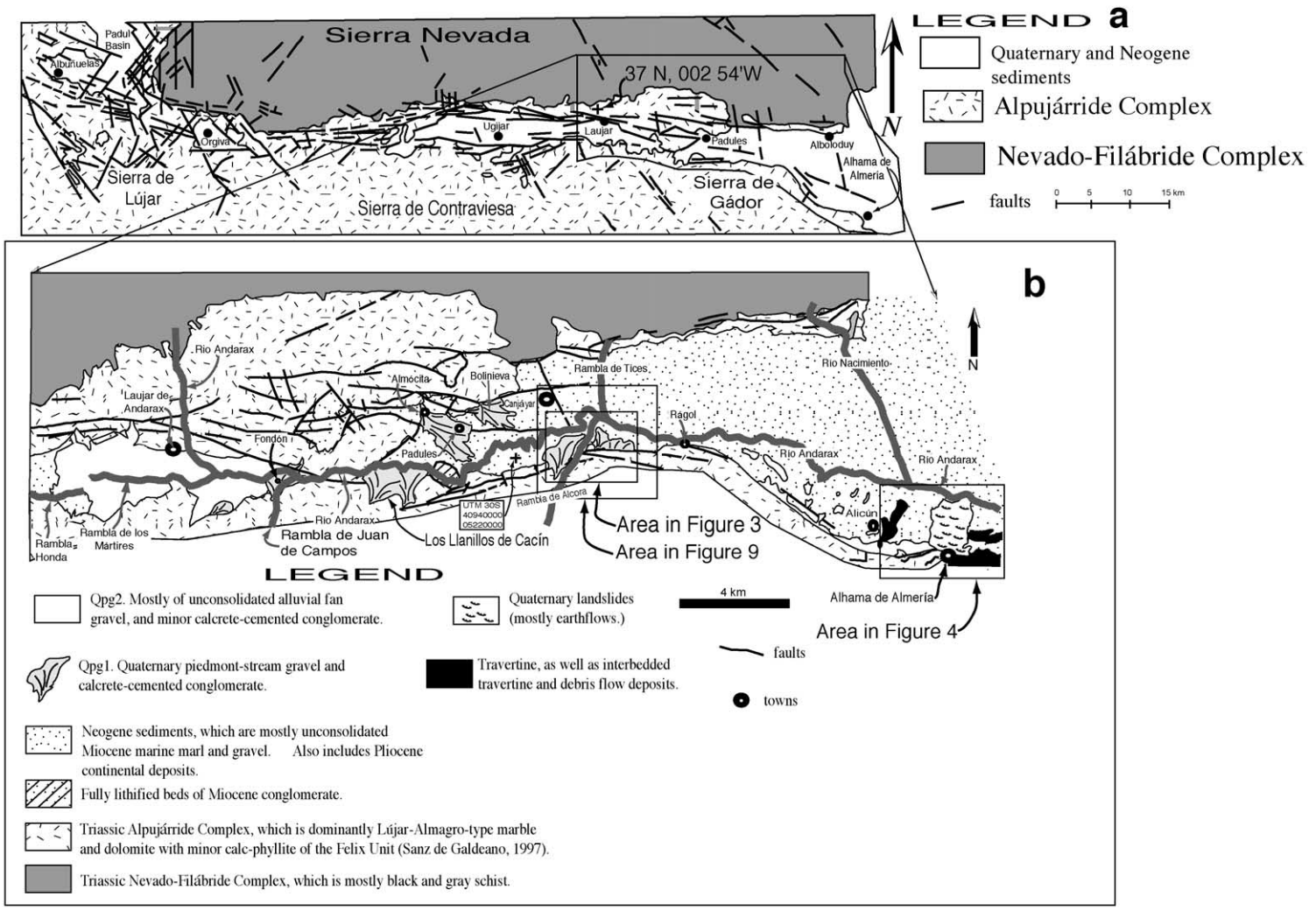

Fig. 2. (a) Generalized geologic map of the Alpujarran Corridor. For the location of this map relative to Fig. 1, note the location of Sierra Nevada and the Alpujarran Corridor. This map is redrawn from Sanz de Galdeano et al. (1986). (b) Generalized geologic map of the eastern Alpujarran Corridor, modified from Sanz de Galdeano et al. (1991). Some Quaternary units are reinterpreted, and some faults are omitted for clarity.

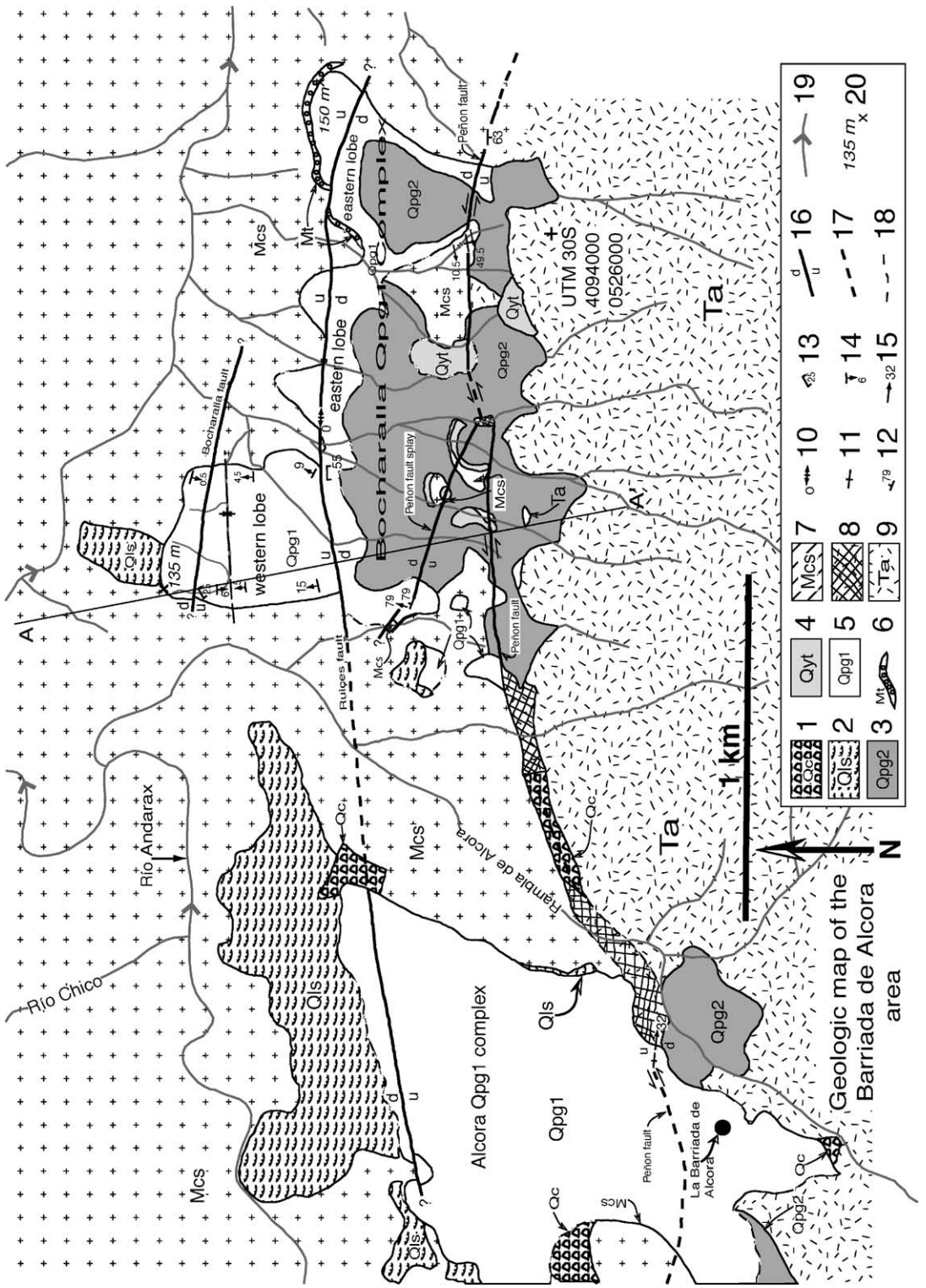
Río Chico
Río Andarax
Mcs
Qls
Qc
Qpg1
Qpg2
Qyt
Ta
Bocharalla Qpg1 Complex
western lobe
eastern lobe
Bocharalla fault
Peñon fault splay
Peñon fault
Ruices fault
Rambla de Alcora
Alcora Qpg1 complex
La Barriada de Alcora
135 m
150 m
A
A'
UTM 30S
4094000
0526000
1 km
N
Geologic map of the Barriada de Alcora area

1991). The Middle Miocene marls are locally unconformably overlain by tan to yellowish, locally silty travertine (Mt; Fig. 3). The travertine beds are 3–5 m thick. At their base, they commonly have inclusion of Middle Miocene marl and are locally interlayered with reworked Middle Miocene marl. Travertine cemented plant material collected from one of these beds yielded an age >350 ka Table 1. On the basis of this radiometric datum, and on the stratigraphic character and position of the travertine beds, their age is inferred as Miocene.

3.3. Plio-Quaternary gravel and conglomerate (PQc)

Near the town of Alhama de Almería, basin-fill sediments are dominantly Plio-Quaternary conglomerate and gravel (PQc, Fig. 4). PQc is fanglomerate, sensu stricto, in that the fluvial network that deposited these sediments no longer exists, and the sediments are substratum that is dissected by the present-day fluvial network. PQc comprises moderately indurated sands and gravels, with minor unconsolidated sands and gravels. North of highway N-324 and south of Río Andarax, PQc is completely indurated conglomerate and completely indurated sedimentary breccia. PQc deposits are up to 100 m thick and their base is not exposed in the mapped area. Based on stratigraphic relationships and regional correlations, Pascual Molina (1997) inferred these sediments to be uppermost Pliocene and lowermost Pleistocene in age. PQc was deposited on the hanging wall of a NW striking normal fault whose trace is about 0.5 km NE of Alhama de Almería (Pascual Molina, 1997).

4. Geomorphology of the EAC

The EAC is a 30-km long and 4–6-km wide E–W trending topographic trough bordered to the north and south by the highest mountain ranges in the Betic Cordillera (Fig. 1). The topographic trough coincides with an inverted Miocene/Neogene sedimentary basin (Figs. 1 and 2). Superimposition of the modern drainage network over the basin led to development of rugged, steep topography within and adjacent to the EAC. Quaternary fluvial denudation resulted in an erosional landscape characterized by prominent, high-level depositional surfaces and multiple inset erosional surfaces (Figs. 2, 6 and 7). Topographic relief from the bottom of the EAC to adjacent mountainous crests is typically between 1000 and 1500 m.

The axial stream of the EAC is the Río Andarax, which an ephemeral stream with a mixed bedrock/alluvial channel. The lower 52 km of the longitudinal profile of Río Andarax is a concave-up and smooth (Fig. 8). A prominent knickpoint about 52 km from the Andarax rivermouth separates the concave-up reach from a convex-up reach. Development of Río Andarax's longitudinal profile, as well as its late-Quaternary incision history, was controlled largely by the passing of a tectonically induced incision wave (García, 2001; see additional discussion below).

The Quaternary geology of the EAC was mapped in detail on 1:12,500 scale topographic base maps (García, 2001), and is dominated by deposits originating from tributaries to the Río Andarax. The most widespread Quaternary sediments in the EAC are calcretized gravel deposits (Qpg1, described in detail below). Another significant Quaternary deposit in the EAC is a sequence of travertine and interbedded fluvial sediments in the Alhama de Almería area ("AdA sequences," which consists of the Qtd and Qt map units, also described in detail below). AdA sequences are significant because Th/U series analyses of travertines provide age control for EAC Quaternary stratigraphy (García, 2001).

Depositional surfaces underlain by Qpg1 and AdA sequences are anomalously low relief, large, high-

Fig. 3. Geologic map of the Bocharalla Qpg1 complex and Alcora Qpg1 complex. Key for map legend: (1) colluvium (Qc); (2) Quaternary landslide (Qls), which includes rotational slumps, translational rock block slides, earthflows and debris avalanches; (3) younger Quaternary piedmont gravels (Qpg2), which are active alluvial fan channels and alluvial fan surfaces; (4) Quaternary younger travertine (Qyt); (5) older, oxygen isotope Stage 8 time Quaternary piedmont gravels (Qpg1); (6) Miocene travertine (Mt); (7) undifferentiated Miocene clastic sediments (Mcs); (8) fault gouge and fault breccia; (9) Triassic Alpujárride Complex (Ta); (10) horizontal striations on vertical fault surfaces; (11) vertical fault surfaces; (12) strike and dip of a fault surfaces; (13) strike and dip of bedding; (14) apparent dip of bedding (arrow indicates the direction of dip); (15) trend and plunge of striations; (16) fault, "d" is the downthrown block, and "u" is the upthrown block; (17) inferred fault trace; (18) inferred location of geologic contact; (19) streams and drainage network (arrows indicate flow direction); (20) height of Qpg1 base above Río Andarax's channel at the location denoted by the ×.

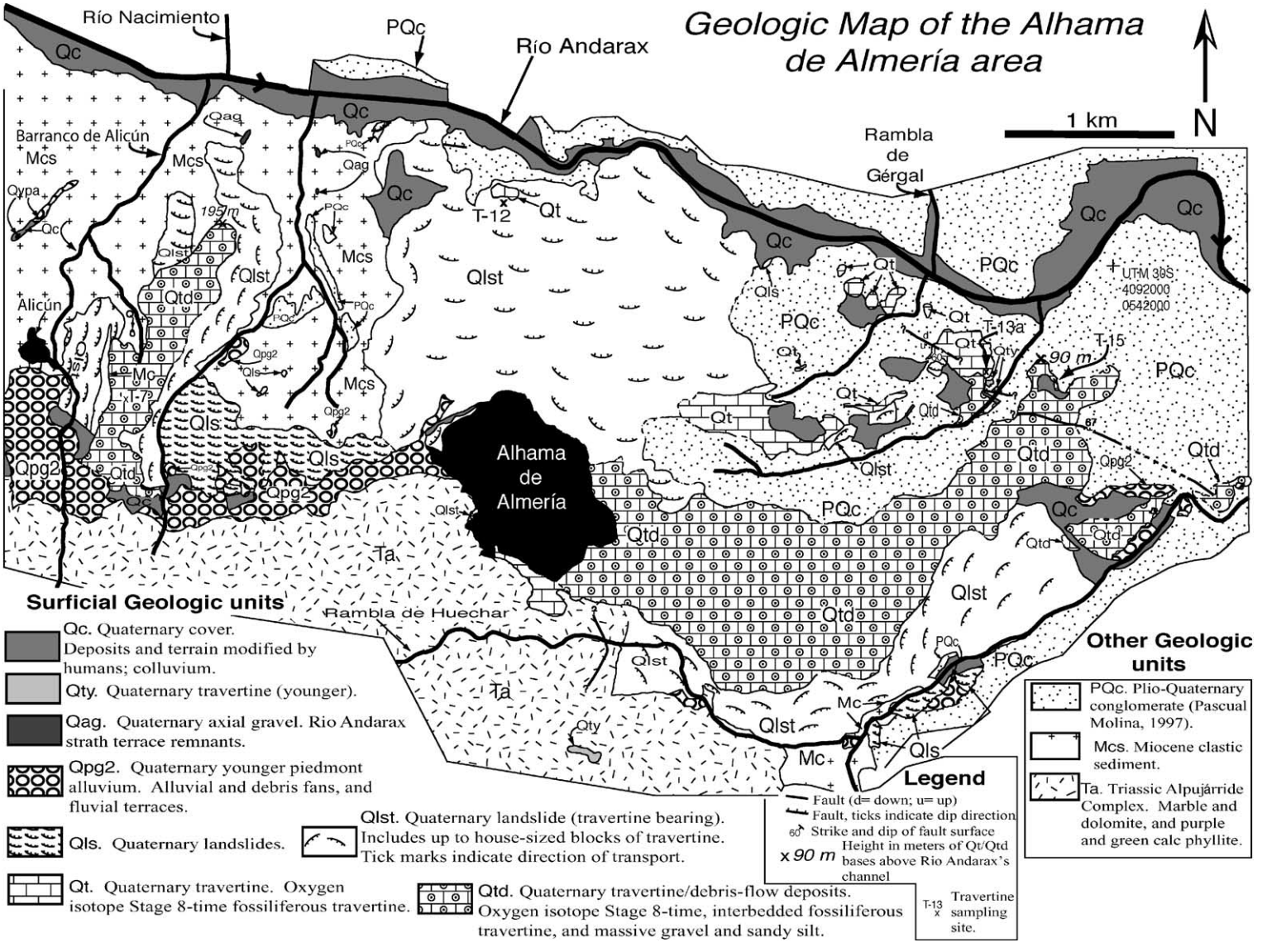

Fig. 4. Geologic map of the Alhama de Almería environs. Qc adjacent to Río Andarax is agricultural terraces.

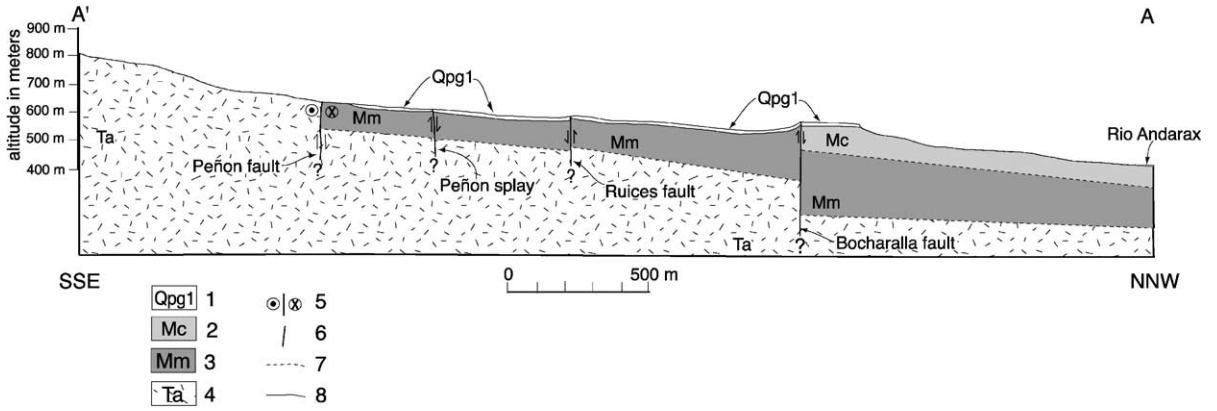

Fig. 5. Geologic cross-section of the western lobe of the Bocharalla Qpg1 complex. The differentiation of Miocene sediments (Serravallian vs. Tortonian and Messinian) is adopted from Sanz de Galdeano et al. (1991). Qpg2 was not included on the cross-section because it is too thin to represent accurately at the scale the cross-section is drawn. The dip of Qpg1 south of and within 10 m of the Bocharalla fault on the cross-section is the maximum steepness measured in the field, and may not be as steep elsewhere along the fault. See Fig. 3 for the location of the cross-section. Legend: (1) Quaternary piedmont gravels (Qpg1); (2) Miocene conglomerate (Tortonian and Messinian; Mc); (3) Miocene marl (Serravallian; Mm); (4) Triassic Alpujárride complex (Ta); (5) left lateral strike-slip fault; (6) fault; (7) inferred geologic contact; (8) geologic contact.

level surfaces that visually dominate the EAC landscape (Figs. 6 and 7). Qpg1 and AdA travertine landform surfaces are unquestionably a paleo-valley floor, and are at the same paleofluvial level (Fig. 6). These two observation-based inferences are supported by results of detailed field mapping, which established the altitude of the bases of Qpg1 deposits throughout the EAC (García, 2001; (Table 2).

The height of AdA travertine sequence and Qpg1 bases above the present-day channel of the EAC axial stream (Río Andarax) is not consistent (Table 2). However, AdA sequences and Qpg1 deposits originate from tributaries and dip towards the Río Andarax, so their distal extremities are eroded by varying amounts. As a result, the present-day AdA travertine and Qpg1 bases nearest to the modern Río Andarax channel do not reflect the position of Río Andarax when they were deposited. The critical data suggesting that the AdA sequences and Qpg1 deposits comprise a common paleofluvial level is the consistently higher altitude of their bases as distance from the mouth of Río Andarax increases (Table 2).

4.1. Geomorphic setting of the study areas

This paper is based mostly on the surficial geology of two areas in the EAC. The study areas are at the northern Sierra de Gádor piedmont, between the towns of Canjáyar and Alhama de Almería (Figs. 2, 6 and 9). The first area straddles a Río Andarax tributary that is known as Rambla de Alcora. Two kilometers east and west of Rambla de Alcora, the Sierra de Gádor's piedmont is dominated by Qpg1 landforms (Figs. 3 and 9). These landforms are herein

Table 1
Th/U analyses of travertine-fossilized plant stems collected in the eastern EAC

Sample, elevation of sampling site, map unit	U (ppm)	$^{234}U/^{238}U$	$^{230}Th/^{232}Th$	$^{230}Th/^{234}U$	Age (ka)
T-7, 540 m, Qtd	0.72 ± 0.02	1.11 ± 0.03	70.5 ± 10.1	0.95 ± 0.03	276 ± 40
T-12, 385 m, Qlst	1.81 ± 0.04	1.01 ± 0.02	168 ± 25	0.97 ± 0.03	354 ± 76
T-13a, 325 m, Qt	1.30 ± 0.03	1.04 ± 0.03	101 ± 16	0.91 ± 0.03	248 ± 29
T-15, 310 m, Qtd	0.89 ± 0.02	1.04 ± 0.02	90.9 ± 12.2	0.94 ± 0.02	282 ± 34
BFC-1, 585 m, Mt	–	–	–	–	>350

Uncertainties are standard deviations derived from counting statistics. Samples T-*n* were collected near Alhama de Almeria (Fig. 10). Sample B-1 was analyzed by Laboratorio de Radiochronologia del Instituto Jaume Almera, CSIC, Barcelona, Spain.

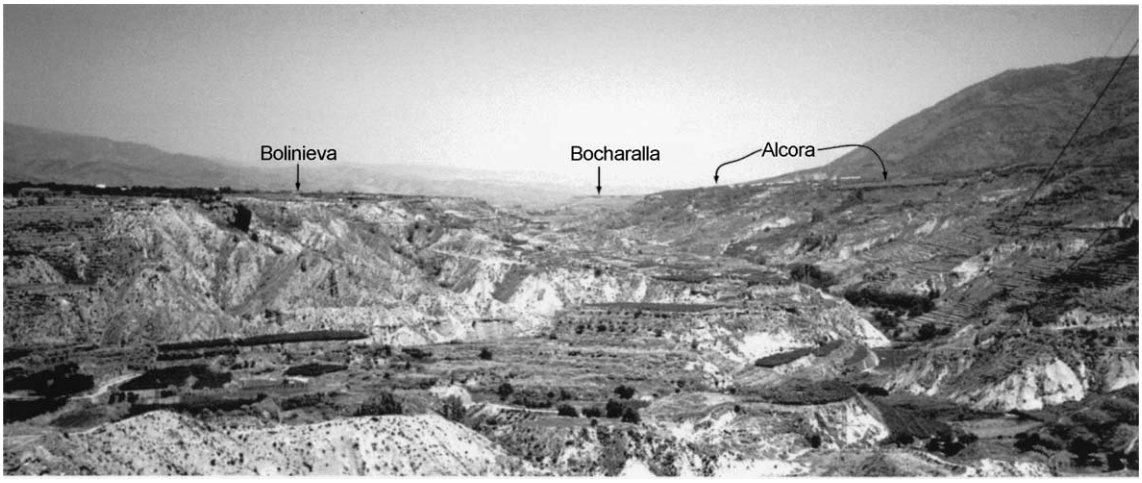

Fig. 6. View to the east from the Padules/Almócita Qpg1 landform surface. See Fig. 2b for the location of the labeled landforms; they are underlain by Qpg1.

referred to as the Bocharalla Qpg1 complex and the Alcora Qpg1 complex (Fig. 3). Here, the Río Andarax is incised up to 150 m below the bases of Qpg1 deposits at the distal part of the Bocharalla Qpg1 complex (Table 2 and Fig. 3). Rambla de Alcora is also incised many tens to hundreds of meters below the bases of Qpg1 deposits. Large landslides are present at the margins of Qpg1 landform treads where streams have incised deeply below the contacts of Qpg1 and Mid Miocene as well as Late Miocene marl. This paper focuses on this area because it includes the only significantly faulted Quaternary deposits in the EAC (García, 2001).

The second area studied in detail is the region near the towns of Alhama de Almería and Alicún (Figs. 2 and 4). The most noteworthy features of the Sierra de

Fig. 7. View to the east of the Sierra de Gádor piedmont in the vicinity of Huécija and Alicún. The towns of Alicún and Huécija are labeled. The feature labeled as "AdA travertine landform" is the N–S elongate Qtd unit about 1 km east of Alicún (Fig. 4).

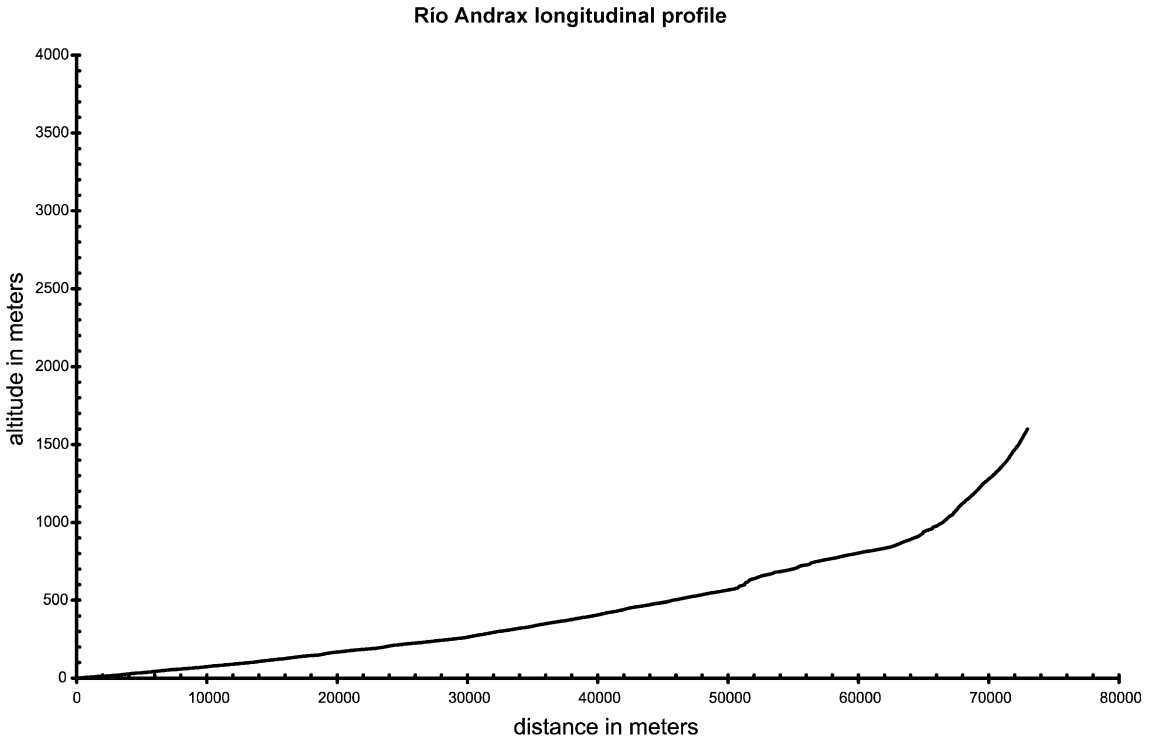

Fig. 8. Longitudinal profile of Río Andarax. The *x*-axis is distance in meters from the Río Andarax rivermouth.

Gádor piedmont in this area are landform surfaces, up to a few square kilometers in area, that are underlain by AdA sequences (Fig. 4). The Río Andarax is incised up to 95 m below the bases of the AdA travertine sequences. Areas between AdA travertine landform surfaces include dissected Miocene and Pliocene sediments and earthflows that are up to a few square kilometers in area (Fig. 4).

5. Quaternary geology and structure of the Rambla de Alcora area

The results of the field investigation that form the fundamental basis of this paper are presented in this section and in Section 6. In these two sections, the geology, sedimentology and structure of the two study areas are described, with emphasis on sediments and structures most useful for deducing the Mid Quaternary to recent history of the EAC. Summary descriptions of other Quaternary map units are presented in Table 3.

5.1. Quaternary geology of the Rambla de Alcora area

Quaternary piedmont gravel, or Qpg1, records the only preserved paleofluvial level in the vicinity of Rambla de Alcora. In this area, Qpg1 is mostly gravel and conglomerate entirely composed of Alpujárride Complex marble and dolomite clasts. The Sierra de Gádor is formed entirely in Alpujárride Complex rocks (e.g., Sanz de Galdeano, 1997), and Qpg1 contains only Alpujárride Complex clasts, and it lacks axial stream Nevado–Filábride clasts. This indicates that Qpg1 was deposited exclusively by Sierra de Gádor piedmont streams.

Qpg1 deposits overlie smooth, locally angular unconformities developed mostly into Miocene sediments and less commonly into Triassic bedrock. At the eastern part of the herein named eastern lobe of the Bocharalla Qpg1 complex (Fig. 3), Qpg1 beds and the pediment they overlie dip between 12° and 19° to the north and away from the Sierra de Gádor mountain front. Within a few hundred meters of the mountain

Table 2
Altitude and height-above-channel data for AdA travertine sequences and Qpg1 deposits

	Alhama de Almería travertine I (Qtd)[a]	Alhama de Almería travertine II (Qt)[a]	Travertine east of Alicún (Qtd)[a]	Bocharalla fan complex[b]	Padules/ Almócita Qpg1[c]	Los Llanillos de Cacín fans[c]	Juan de Campos fan[c]
Distance from river mouth (km)	24.1	24.8–25.1	28.8	41.4–42.9	50.0–50.8	52.9–55.4	58.6–60.0
Plan-view distance of data (μm) from Rio Andarax's channel (m)	375	144–250	>500	194–338	263–325	75–81	–
Altitude of deposit base (m)	300	300	395[d]	590	710–715	710–765	<780–<800
Height of base above Rio Andarax (m)	95	65	155[d]	160–145	145–135	25–80	<0 (base not exposed)
Maximum rate of Rio Andarax incision since ois8[e] (m/ka)	0.4	0.3	0.6	0.7–0.6	0.6	0.3–0.1	–

[a] See Figs. 3 and 10.
[b] See Figs. 3 and 5.
[c] See Fig. 3.
[d] Calculated by projecting from the axial-streamward edge of the deposit to the present-day position of Rio Andarax's channel using the slope of the deposits tread.
[e] ois8 = oxygen isotope Stage 8 glacial maximum; eustatic fluctuation had a negligible effect on stream incision on these reaches of Rio Andarax (García, 2001). Rates calculated by dividing height above Rio Andarax's channel by 245 ka, which is the end of ois8 (Imbrie et al., 1984).

front the deposits are up to 5 m thick and are on average about 3.5 m thick. They are up to 30 m thick at the most distal part of the eastern lobe.

Adjacent to and east of Rambla de Alcora (herein named the "western lobe of the Bocharalla Qpg1 complex"; Fig. 3), in most areas that are 100 m or farther away from faults, Bocharalla Qpg1 deposits dip from 5° to 15° to the north and away from the Sierra de Gádor mountain front. At the distal part of the western lobe, Qpg1 beds dip 0.5–6° to the south (toward the mountain front). The variable dip of the deposits on the western lobe are interpreted to reflect deformation (see below). Qpg1 deposits of the western lobe are typically 10–15 m thick within 1–200 m of the mountain front and are typically 7–10 m thick at the most distal part of the deposits.

The morphostratigraphic character of Qpg1 deposits west of Rambla de Alcora (the "Alcora Qpg1 complex") is similar to the morphostratigraphic character of the Bocharalla Qpg1 complex western lobe (Fig. 3). Alcora Qpg1 complex sediments locally bury paleotopography proximal to the Sierra de Gádor mountain front. Farther away from the mountain front, Alcora complex Qpg1 gravels are 5–15 m thick and overlie a very smooth unconformity.

The sedimentologic description that follows was made approximately 650 m from the Sierra de Gádor mountain front. Clast sizes are reported as median diameters and are generally larger (up to 1.5 m) closer to the mountain front and smaller farther from the mountain front. Qpg1 consists of lenticular beds of crudely sorted, clast supported, massive and stratified, subangular gravels and silty sands. The width of lenticular beds varies from 1 to 12 m and their thickness varies from 0.2 to 1.5 m. Clasts in these beds are typically less than 5 cm, but as large as 18 cm. The lenticular beds are interbedded and interfingered with beds consisting of poorly sorted, matrix supported, massive, subangular gravels supported within a sandy–silt matrix. These matrix-supported beds are laterally continuous across outcrops as wide as 15 m. Clasts in matrix-supported beds are up to 15 cm but typically less than 10 cm. Buried soils are locally common within this Qpg1 sequence.

5.2. Bocharalla and Alcora Qpg1 complex depositional environments

The interbedded and interfingered lenses of clast-supported gravel and beds of matrix-supported gravel

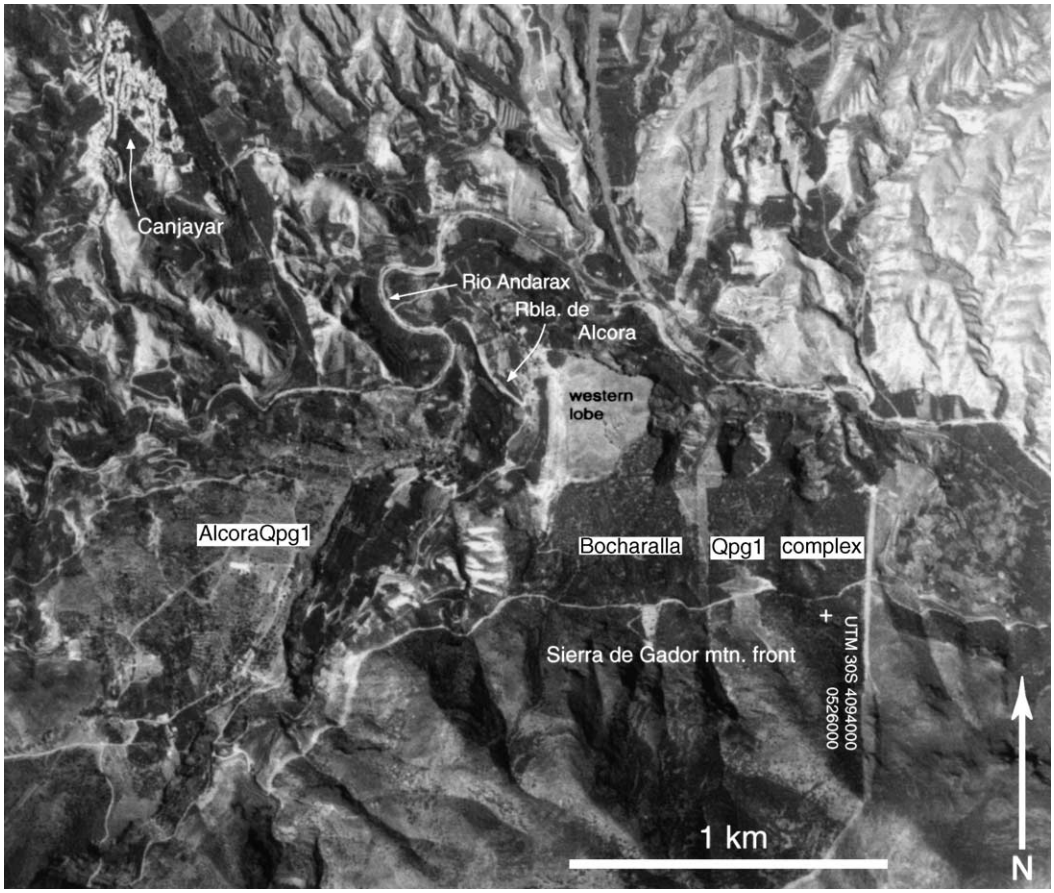

Fig. 9. Aerial photograph of the Rambla de Alcora area. Canjáyar is at the northwest corner of the photo. The north-trending white line east of the word "complex" is a treeless fire break. The photo was provided by Instituto Geográfico Nacional de España/Centro Nacional de Información Geográfica (Spain) (used with permission from Centro Nacional de Información Geográfica, Spain).

typical of Qpg1 deposits indicate alternating fluvial and debris flow deposition typical of an alluvial fan environment (e.g., Harvey, 1990). The morphostratigraphic character of the eastern lobe of the Bocharalla Qpg1 complex indicates that it is an alluvial fan deposit that overlies an erosional pediment surface.

Interpretation of the depositional environment of the Alcora Qpg1 complex and the western lobe of the Bocharalla Qpg1 complex is not as straightforward. The morphostratigraphic character of Qpg1 deposits that comprise the western lobe of the Bocharalla Qpg1 complex and the entire Alcora Qpg1 complex (Fig. 3) indicate that they were deposited by piedmont streams on pediments and straths. The Bocharalla Qpg1 complex and the Alcora Qpg1 complex are fan-like in plan view (Fig. 3) and are similar to a pediment gravel in that their bases and treads diverge from the present-day stream channel. They are strath terrace like in cross-section, in that they overlie very smooth unconformities along a substantial length (0.5–1.5 km) of a large stream. This paradoxical character is typical of Qpg1 deposits throughout the EAC (García, 2001). Unfortunately, "case hardening" of Qpg1 outcrops precludes sedimentologic analyses that would facilitate classifying the western lobe of the Bocharalla Qpg1 complex and the Alcora Qpg1 complex in a conventional landform classification scheme.

Table 3
Summary description of Quaternary map units younger than Qpg1 and AdA sequences

Map unit *	Map unit name	Sedimentology/morphostratigraphy	Additional notes
Qc	Quaternary cover	Quaternary cover. Includes colluvium, and landforms obliterated by human activity.	Includes fruit orchards on gently sloping surfaces.
Q1st	Quaternary landslide with travertine blocks	Earthflows and slumps. Q1st is mostly earthflows consisting of blocks of travertine that are typically 10 s of m^3 and up to 100 s of m^3 in a 'matrix' of Miocene and Quaternary marl. A fossil plant stem collected from a travertine block in Q1st yielded an age of 354 ± 76 k.y. (Table 1).	Active and inactive slope failures.
Q1s	Quaternary landslide	Earthflows and slumps. Most common at the edges of the Bocharalla Qpg1 complex and the Alcora Qpg1 complex where streams have incised 50 m or more below the contact of Qpg1 and Miocene sediments (Fig. 3).	Active and inactive slope failures.
Qag	Quaternary axial-stream gravel	Qag sediments are poorly indurated to unconsolidated, well stratified and/or imbricated, clasts-supported gravel that is locally massive, and up to 7 m thick. Based on the unpaired nature of these terrace remnants, and on the great variability in their heights, Qag deposits are interpreted as complex response/minor strath terraces (*Sensu* Bull, 1990).	Unpaired strath terraces.
Qpg2	Quaternary piedmont gravel 2	Unconsolidated, colluvial and alluvial gravel, sand, and minor silt. The gravel is dominantly clasts of bluish-black Alpujárride marble and dolomite, and includes common fragments of caliche rubble. The clasts are dominantly angular to subangular, and include very minor amounts of sub-rounded and rounded clasts. Qpg2 sediments are active debris fan, alluvial fan, and alluvial-distributary channel deposits.	Based on the limited areal extent of Qpg2 in the EAC, we interpret these sediment as a "minor" or "complex response" deposits (sensu Bull, 1990; García, 2001).
Qyt	Quaternary younger travertine	Tan to gray, locally silty, and massive travertine. Rings sharply and distinctively when struck with a hammer. The deposits form arcuate outcrops that are tens of meters in length by ten to twenty meters wide, and bean shaped outcrops that are 10 to 100 m wide. Present slightly upslope and mostly downslope of faults. The age of these travertine deposits is inferred, and is based on landscape and stratigraphic position.	Probably formed as a result of groundwater discharge from faults and fractures.

* Map units are listed from youngest (top of the table) to oldest. Ages are relative and inferred from landscape position.

5.3. Calcretes in the Alcora Qpg1 complex and Bocharalla Qpg1 complex western lobe

The surfaces of the Bocharalla Qpg1 complex western lobe and of the Alcora Qpg1 complex are formed by coarsely and densely crystalline, fully lithified calcrete. The caliche rubble typical of alluvial fan calcretes in southern Spain (Alonso-Zarza et al., 1998) is not present on either the Bocharalla Qpg1 complex western lobe or the Alcora Qpg1 complex. Instead, their surfaces are dominated by microkarst towers that are 20–50 cm high (García, 2001). The macromorphological attributes of the Bocharalla and Alcora Qpg1 complexes indicate that they are groundwater calcretes (García, 2001).

The petrography of the western lobe calcrete (Fig. 10) is consistent with interpretations based on macromorphology. Microfabric features that are typical of pedogenic calcretes in other parts of southern Spain are absent. García (2001) showed that the character of the micofabric is, however, typical of groundwater calcrete microfabrics as outlined in Wright and Tucker (1991) and similar to groundwater calcretes in the nearby Tabernas basin of SE Spain described by Nash and Smith (1998).

5.4. Calcretes in the eastern lobe of the Bocharalla Qpg1 complex

The surface of the eastern lobe of the Bocharalla Qpg1 complex is similar to the "Stage 6a" fan surfaces as described by Alonso-Zarza et al. (1998), in that laminar calcrete is exposed in some areas and other areas are mantled by caliche rubble. This suggests that the calcrete is pedogenic, but micromorphology suggests more complex calcrete development (García, 2001). Calcrete petrography of two samples collected from the eastern lobe of the Bocharalla Qpg1 complex indicate calcrete formation in a pedogenic environment, followed by cementation and calcretization in a groundwater environment (Fig. 11; García, 2001).

5.5. Landscape evolution and relative age implications of Bocharalla Qpg1 complex calcrete morphology

Like the Bocharalla eastern lobe pedogenic calcrete, the Bocharalla western lobe had a pedogenic calcrete above a groundwater calcrete (García, 2001). The western lobe calcrete, therefore, reflects a relatively advanced state of landform development,

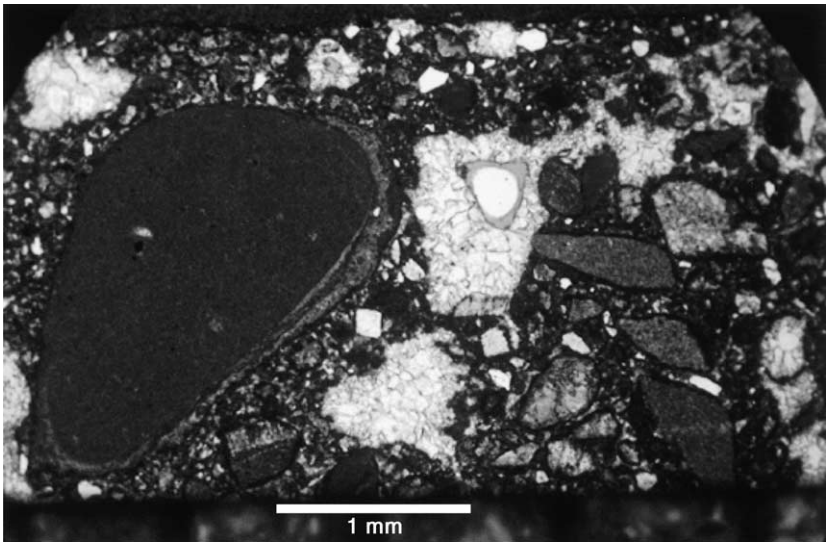

Fig. 10. Petrographic thin section of sample B-3 under plain light. The translucent, coarsely crystalline areas are pore spaces filled with spar. The gray area, which engulfs an ellipsoidal white area and is within the spar-filled pore space, is a pore space stained with blue dye. Most clasts have well-developed micritic rims. For example, the alternating dark and light bands that form a thick rim on the upper right of the largest clast are spar (light bands) and micrite (dark bands).

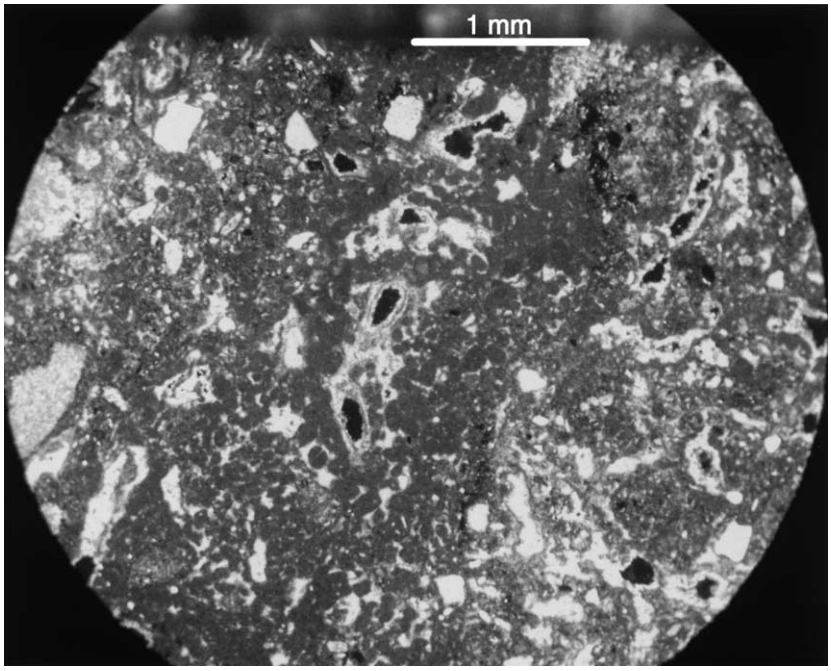

Fig. 11. Petrographic thin section of sample B-2 under plain light. A cluster of micritic glaebules form a diagonal band across the view in the photo. The band is in a matrix of micrite and spar, which is in the upper left and lower right of the photo.

wherein its soil profile has been stripped. The calcrete of the eastern lobe of the Bocharalla Qpg1 complex is less degraded than the calcrete of the western lobe, in that it is mantled by caliche rubble, and the microfabrics of calcretes on the eastern lobe include features associated with pedogenic calcrete.

The western and eastern lobe Qpg1 gravels are physically continuous (Fig. 3), so differences in their calcrete crusts must arise from a factor other than the depositional age of Qpg1. Sediment supply to the western lobe was cut off shortly after the end of ois8, when the Rambla de Alcora incised below the western lobe surface (García, 2001). The eastern lobe is fed by streams originating from relatively small mountain front catchments that have not incised below its tread. In fact, the proximal Qpg1 calcrete on the eastern lobe of the Bocharalla Qpg1 complex is buried by recent alluvium (Qpg2; Fig. 3) originating from these catchments. Since the distal part of the lobe still receiving sediment, albeit in limited supply, its pedogenically calcretized surface has been a stable feature over Quaternary time scales (Alonso-Zarza et al., 1998). The relatively well-preserved character of the eastern lobe calcrete is due to its proximity to the Sierra de Gádor mountain front and to the relatively small catchment area of streams that feed the lobe.

5.6. Structure of the Bocharalla and Alcora Qpg1 complexes

The only significant Quaternary faults in the EAC are described in detail in Section 5.6. The faults are on the south side of the EAC, within 1 km of the Sierra de Gádor mountain front. Quaternary faults within this part of the Betic Cordillera were previously unrecognized. One purpose of this section is to establish the character of the Late Quaternary faults in the EAC, for later discussion regarding the character of Mid/Late Quaternary faulting in the EAC within the framework of Betic Cordillera Quaternary tectonism. Another purpose of this section is describing the style and magnitude of Quaternary faulting for subsequent discussion regarding the role of faulting in EAC landscape development.

The faults and fault zones present in the Bocharalla and Alcora Qpg1 complexes are mostly vertical and

slip on faults is mostly oblique. Localized areas of normal faulting are present, but the main fault strands of fault zones are vertical. Along these main fault strands, fault surfaces are locally subvertical, but these are irregularities, and the faults are vertical at outcrop scales. Their displacements cannot be described in terms of hanging walls or footwalls and, therefore, the faults are described as "south-side up or "north-side up." The faults are described in detail below and are listed from north to south. Names of faults are taken from names that appear close to the surface trace of each fault on the Padules (1044-I) and Canjáyar (1029-III) sheets of the Mapa Topográfico Nacional de España, 1:25,000 scale series.

5.6.1. Bocharalla fault

The Bocharalla fault is vertical, strikes ESE and deforms Qpg1 at the distal, western lobe of the Bocharalla Qpg1 complex (Figs. 3 and 5). It is best exposed on a road cut at the western, N-trending edge of the distal western lobe, where the contact of Qpg1 and Miocene marl is vertically displaced a minimum of 2.3 m (south-side up). Also at this locality, south and within 50 m of the fault, Qpg1 beds deformed by the Bocharalla fault locally dip 25° to the southeast. As mapped in this study, the Bocharalla fault deforms Miocene gravel at its eastern end and is 730 m long (measured from a 1:12,500 scale field map with a digital planimeter). Sanz de Galdeano et al. (1991) mapped this fault as the local contact between Middle Miocene sands and gravels and Middle–Late Miocene marls. Their map depicts the Bocharalla fault trace in Miocene sediments from the town of Padules, to 3.5 km east of the western lobe, which is a distance of approximately 8 km (Fig. 2).

5.6.2. Cortijo de los Ruices fault ("Ruices fault")

The Ruices fault is vertical, strikes E to ESE and ENE, and deforms the western and eastern lobes of the Bocharalla Qpg1 complex (Figs. 3 and 5). In the eastern lobe, the Ruices fault displaced the contact of Qpg1 and Miocene marls 9.5 m with a dip slip, north-side up sense of movement. Qpg1 beds dip southward as steeply as 55° at an exposure about 50 m south of the Ruices fault. Along its entire length on the Bocharalla Qpg1 complex surface, the Ruices fault forms a 3 to 5 m high fault scarp that is moderately degraded (Fig. 12). The Ruices fault is locally a fault zone with fault surfaces that are spaced less than 10 m and up to 15 m apart, and includes a graben. A vertical fault surface formed in Qpg1 within this graben strikes 91° and has horizontal striations. The Ruices fault is moderately well-exposed at the northwestern edge of the Alcora Qpg1 complex. At this locality, it is a south-side up, high-angle fault, and the Qpg1–Miocene contact is vertically displaced by approximately 7 m. The Ruices fault is an oblique-slip fault that changes sense of dip-slip displacement along strike, as indicated by the following observations: (1) horizontal striations on a fault surface formed in Qpg1; (2) the vertical offset of Qpg1 gravel; and (3) the along-strike change in sense of separation (north side up vs. south side up). The total length of the fault and fault zone is 3.3 km.

5.6.3. Vereda del Peñon fault ("Peñon fault")

The Peñon fault is a 4.4-km long segment of a mostly vertical system of faults that locally defines the southern boundary of the Alpujarran Corridor (Sanz de Galdeano et al., 1991). In the study area, it strikes E to NE, juxtaposes Miocene sediments and Triassic bedrock, and is locally developed as an intra-Alpujárride Complex fault and an intra-Miocene marl fault (Figs. 3 and 5). The trace of the Peñon fault is locally defined by bands of fault breccia up to one hundred meters wide formed in Triassic bedrock and Miocene sediments. In the Bocharalla Qpg1 complex, the Peñon fault is mostly buried by younger alluvium (Qpg2, Fig. 3), but it is exposed in stream channels. Displacement on the Peñon fault in the Bocharalla Qpg1 complex is south-side up, and at one locality in a stream channel within the Bocharalla Qpg1 complex, striations on a vertical fault surface formed in Miocene marl have the following trends and plunges: 235°, 10.5° and 235°, 49.5°. Because it is a south-side up fault, these data support the notion of left lateral oblique separation on this fault since Neogene time. At this same locality, another fault surface formed in Miocene sediments has an attitude of 079°, 81°S. The Peñon fault does not deform Bocharalla–Qpg1 complex sediments.

At the zone of gouge and breccia that constitutes the Peñon fault where it intersects the eastern end of the Alcora Qpg1 complex (Fig. 3), Qpg1 gravels are vertically displaced a minimum of 8 m, with north-side up separation. Poor exposure precludes determin-

Fig. 12. View to the east of an exposure of the Ruices fault. The net displacement across this vertical fault zone is north-side up. The surface trace of the main fault strand is at the southern base of the hill in which the faults are drawn in black; the hill is a fault scarp. The north–south distance between the trace of the main strand and the fault drawn in white is approximately 30 m. The fault scarp in this photo is present along the entire surface trace of the Ruices fault on the tread of the Bocharalla Qpg1 complex. All sediments in the view are Qpg1.

ing stratigraphic separation more precisely. A fault surface formed in gouge and breccia, near to where the 8 m of north-side up separation was measured, strikes 94° and is vertical. The trend and plunge of striations on this fault plane are 94°, 32°. Because it is a north-side up fault, these observations indicate that left-lateral oblique separation has taken place on this fault. In addition, the sense of dip-slip displacement in the exposure at the Alcora Qpg1 complex is different from the sense of dip slip displacement in the Bocharalla Qpg1 complex.

5.6.4. Peñon fault splay

A splay of the Peñon fault intersects the main strand of the Peñon fault at a zone of fault breccia and gouge (Figs. 3 and 5). The splay is north of the Peñon fault and it strikes ESE. At its western end, the Peñon fault splay terminates in a complex fault zone that deforms Qpg1. The fault zone includes two principal, north-dipping fault surfaces. The attitude of one of the fault surfaces in Miocene marl within the fault zone, is 110°, 79°N. The trend and plunge of striations on this fault surface are 20°, 79°. There are also drag folds in Qpg1 on the hanging wall, adjacent to the northernmost strand of the complex fault zone. The down to the north displacement of the base of Qpg1 and the striations on the fault plane indicate that the fault zone includes normal faults. Poor exposure precludes determining the amount of dip-slip displacement of the Qpg1–Miocene contact at this normal fault, but is estimated as 6–10 m of normal separation. The Peñon fault splay is 725 m long.

6. Geology of the Alhama de Almería environs

Travertine and related deposits in the Alhama de Almería area (“AdA sequences”; Qtd and Qt in Fig.

4) are at the eastern end of the Alpujarran Corridor (Figs. 2 and 4). These deposits are critical to this study because Th/U series analyses of fossil plant stems collected from AdA sequences provide age control for the Quaternary geology of the EAC.

6.1. AdA sequences (Qtd and Qt)

Qtd (Fig. 4) consists of sequences of interbedded sediments and travertine. The Qtd sequences include decimeter to meter thick beds of travertine, fossiliferous travertine, silt and sand, as well as stratified and massive gravel (Fig. 4). The sequences are typically 10–20 m thick and are capped by travertine, and the surfaces of landforms underlain by Qtd sequences are formed by travertine. Qtd sequences overlie smooth unconformities cut into Mcs and PQc and dip gently away from the local Sierra de Gádor mountain front.

Qtd travertine strata are locally lenticular and consist of alternating reddish, ochre and lavender, massive beds. The beds are typically between 0.4 and 0.7 m thick, but up to 2 m thick and are locally highly fossiliferous. Fossils in the travertine are cylindrical, elongate plant stems that have diameters of a few mm and lengths of a few centimeters. The fossil plant stems are typically horizontal, and their trends are parallel to paleotransport directions inferred from bedding attitude. In Qtd, travertine beds are interbedded and interfingered with lenses of massive, poorly sorted, matrix supported, but locally stratified and clast-supported gravels. The median diameters of gravel clasts are between 0.5 and 40 cm. Massive, lavender to blue, silt and fine sand beds are also present in Qtd, and locally contain abundant fossil plant stems (bioclastic packstone). The dimensions and geometry of the gravel, silt and fine sand beds are similar to the dimensions of the travertine beds. Qt deposits (Fig. 4) are similar to Qtd deposits, but clastic sedimentary beds are rare and are present only as basal beds.

6.2. AdA sequence depositional environment

The depositional environment of the AdA sequences is deduced by studying the present day travertine-fossilization of plant stems in the Alhama de Almería environs and from the sedimentologic character of the clastic sedimentary beds in Qtd. Near Alhama de Almería, plant stems presently being fossilized in the channels of spring-fed streams are oriented with their long axes parallel to stream flow directions (García, 2001). The long axes of fossil plant stems in AdA sequences trend parallel to paleotransport direction inferred from bedding attitude. The trend of the travertine-fossilized plant stems and sedimentologic character of the beds in which they occur, strongly suggests that AdA sequence travertine beds formed in stream channels (cf. Crombie et al., 1997; García, 2001). The massive silt and fine sand beds are interpreted as debris flow deposits derived from phyllite and calcschist of the Felix Unit of the Alpujárride Complex. This interpretation is based on the distinctive lavender and bright blue color of both the Felix Unit and the silt and fine sand beds. Likewise, the poorly sorted, dominantly massive and matrix-supported character of gravel beds also indicates that they are debris flow deposits.

The sedimentologic character of Qtd, most notably the abundant debris flow deposits, indicate that it was deposited by a fluvial and/or alluvial fan system (García, 2001). The dip of AdA sequence beds, which is always away from the local Sierra de Gádor mountain front and toward Río Andarax, indicates that they are associated with Andarax tributary streams. Furthermore, the relationship of Rambla de Huéchar to the largest Qtd landform in Alhama de Almería area (Fig. 4) strongly suggests that Rambla de Huéchar was the source of the debris flow deposits in the Qtd sequences. The Rambla de Huéchar drainage basin south of Alhama de Almería is largely underlain by Felix Unit rocks (IGME, 1980), which is the likely source of the massive silt beds in Qtd sequences. A similar relationship exists between the N–S elongate Qtd landform 0.5 km east of Alicún. Here, the Barranco de Alicún is the likely feeder stream for that Qtd landform, and its drainage basin is partly formed in a Felix Unit thrust sheet (Fig. 4; IGME, 1980). Th/U analyses of a travertine-fossilized plant stems collected from Qtd deposits yielded ages of 276 ± 40 ka (Sample T-7, Table 1) and 282 ± 34 ka (sample T-15, Table 1). A fossil plant stem collected from Qt yielded an age of 248 ± 29 ka (sample T-13a, Table 1).

6.3. Weathering profiles in Qtd and Qt

The AdA sequence landform surfaces are significantly altered by human activity, which precludes

meaningful analyses of calcrete crust morphology or soil formation. In most cases, the surfaces of AdA sequence landforms are formed by exhumed and weathered travertine beds. Soil cover and calcrete crusts are absent.

6.4. Structure of the AdA travertine

A fault system that deforms AdA sequences is present in the northeastern part of Alhama de Almería's environs (Fig. 4). The faults are high angle to vertical and they disrupt and tilt AdA sequence beds. Quaternary dip slip and strike-slip displacement on these faults is negligible (García, 2001).

7. Geochronology and interpretation of mapping results

7.1. Eastern Alpujarran Corridor Quaternary geochronology

Geochronologic data are important to this study because they set EAC Quaternary deformational style in the context of Quaternary deformation elsewhere in the Betic Cordillera. Geochronologic data are also useful for determining rates of fluvial incision, which in turn are used to estimate rates of rock uplift in the EAC. Three types of data and lines of reasoning are used to determine the numeric ages of AdA sequences and Qpg1: (1) a numeric age for AdA sequences is established by Th/U series dating of travertine-fossilized plant stems together with morphostratigraphic relationships, and the numeric age of Qpg1 is based on correlation to AdA sequences (García, 2001); (2) the numeric ages of AdA sequences and Qpg1 are evaluated in the context of established models of climatically driven cycles of fluvial aggradation and degradation; and (3) the degree of calcrete crust development is used to estimate the minimum age of Qpg1.

Numeric age control for EAC geochronology is based on Th/U series analyses of travertine samples collected from AdA sequences (Fig. 4). Three of the four ages yielded by travertine-fossilized plant stems collected in the Alhama de Almería environs are mostly within oxygen isotope Stage 8 ("ois8," which is from 303–245 ka; Imbrie et al., 1984; Table 1 and Fig. 13). The pre-ois8 sample was collected from a

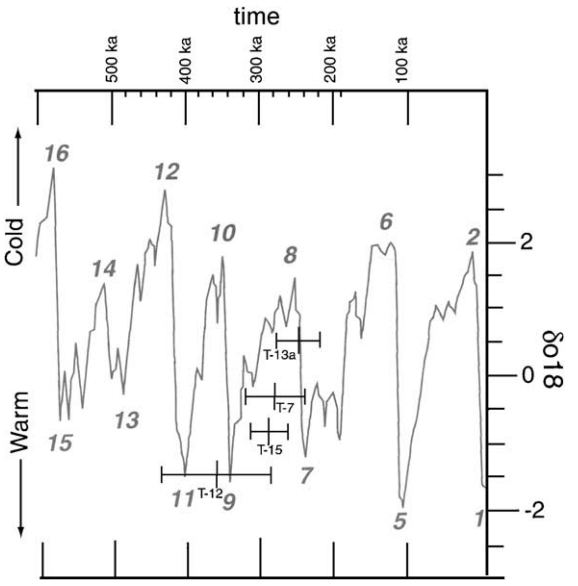

Fig. 13. Plot of oxygen isotope data vs. time (gray curve), with a plot of the ages of the four Alhama de Almería area travertine samples superposed (black symbols). The vertical axis of the age data is arbitrary. The vertical lines at the center of the age plot symbols indicate the determined ages, and the vertical lines at the ends of the age plot symbols indicate the age range within the error of analyses. Numeric age data are listed in Table 1. The vertical axis values of the oxygen isotope plot are units of standard deviation from a normalized mean. The gray numbers are oxygen isotope stages. The oxygen isotope data vs. time plot is modified from Williams et al. (1988).

travertine block within an earthflow 1 km north of Alhama de Almería and yielded an age of 354 ± 76 ka (Fig. 4; sample T-12). The morphostratigraphic relationship of the sample T-12 earthflow to nearby AdA sequence landforms indicates that the earthflow is older than the landforms samples T-7, T-13a and T-15 were collected from. Therefore, the morphostratigraphic character of the sampled travertine deposits is consistent with numeric age data, which indicate that the sample T-12 (354 ± 76 ka) is older than samples T-7 (276 ± 40 ka), T-13a (246 ± 29 ka) and T-15 (282 ± 24 ka; Table 1). These geochronologic results indicate that the age of the AdA sequences coincides with the oxygen isotope Stage 8 glacial maximum (García, 2001).

The numeric age of Qpg1 is based on the numeric age of AdA sequences. AdA sequences and Qpg1 are chronostratigraphically correlated on the basis of similar landscape position (García, 2001). The nu-

meric ages of AdA sequences and Qpg1 are also based on models of climatically induced cycles of fluvial aggradation and degradation in the EAC (García, 2001) and southern Spain (e.g., Harvey, 1990). Fluvial systems in southern Spain aggraded during glacial periods and incised during interglacial periods (e.g., Harvey, 1990; Harvey et al., 1999). Many studies showed that in southern Spain, the Mid Pleistocene was a 'maximum' time of fluvial aggradation and alluvial fan building (e.g., Harvey, 1990). Aggradation was prevalent because of abundant sediment supply in stream catchments (Harvey, 1990). The sedimentologic character of AdA sequences attests to their fluvial origin and their depositional age is a glacial period (ois8) during the Middle Pleistocene fluvial-aggradation maximum (Middle Pleistocene: 780–200 ka.; Berggren et al., 1995). AdA sequences and Qpg1 occupy the highest landscape position within the EAC and they are on the same paleofluvial level (Fig. 14; García, 2001). These relationships, set in the context of models of climatically driven cycles of fluvial aggradation and degradation in southern Spain, strongly suggest that both the AdA sequences and Qpg1 were deposited during ois8 (García, 2001). This conclusion is consistent with the numeric age of travertine overlain by Qpg1 at the Bocharalla Qpg1 complex, which is >350 ka (sample BFC-1; Table 1).

Estimates of the age of Qpg1 based on calcrete-crust morphology are consistent with the correlated numerical age of Qpg1. Although the Bocharalla Qpg1 complex western lobe calcrete does not fall into existing classification schemes (e.g., Machette, 1985; Alonso-Zarza et al., 1998), the eastern lobe calcrete is a Stage 6a calcrete as defined by Alonso-Zarza et al. (1998). Age estimation based on Stage 6a massive calcretes like those of the eastern lobe of Bocharalla Qpg1 complex indicate a pre-latest glacial age (Alonso-Zarza et al., 1998). This age is consistent with the Qpg1 numeric age determined by correlation with the AdA travertine.

7.2. Vertical stream incision since oxygen isotope Stage 8

The altitudes of Qpg1 and AdA sequence bases were determined by detailed field geologic mapping (Table 2; see Section 4) and are interpreted to reflect the ois8-time paleofluvial level in the EAC. Differences in the altitude of the ois8 paleofluvial level and the local altitude of Río Andarax are used to estimate the ois8-time to present incision rate of Río Andarax.

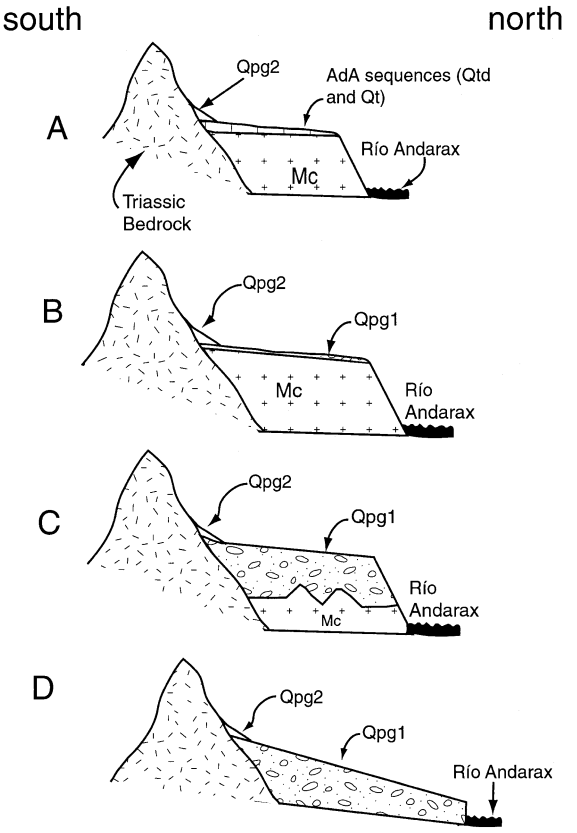

Fig. 14. Schematic diagram of the geomorphic positions of Qpg1 landforms east of Fondón (west of Fondón Qpg1 is present only as partly exposed fan remnants), and of the Alhama de Almería sequences. The diagrams represent the geology of the following areas: (A) Alhama de Almería environs; (B) Bocharalla, Alcora and Padules/Almócita; (C) Los Llanillos de Cacín; (D) Rambla de Juan de Campos fan, near Fondón (see Fig. 2 for the location of the areas).

The maximum magnitude of Río Andarax incision is estimated from the ois8-time paleofluvial level preserved in tributary stream sediments (Qt, Qtd and Qpg1). Vertical distances from Qpg1 and AdA sequence bases to Río Andarax's channel were measured at the toes of landforms underlain by Qpg1, Qtd and Qt (Table 2; Figs. 3 and 4). The measurements were made from 10 m contour lines on 1:12,500 scale surficial geologic maps of Qpg1 and AdA sequences (García, 2001). Incision rates are calculated assuming

that Río Andarax did not incise below the Qpg1/AdA sequence paleofluvial level until the end ois8 (García, 2001). AdA sequences and Qpg1 bases are between 65 and 160 m above the present-day Río Andarax channel and incision rates calculated by dividing these distances by 245 ka (the end of ois8), range from 0.3 to 0.7 m/ka (Table 2). The rates are maxima because Qpg1, Qtd and Qt deposits dip toward Río Andarax and toes of landforms underlain by these deposits are cut back by erosion. Therefore, the present altitudes of Qpg1/AdA sequence bases are slightly above the ois8-time position of Río Andarax. The plan-view distances from the bases of the landforms to Andarax's channel were measured on 1:12,500 scale base maps using a digital planimeter and are shown in Table 2.

7.3. Style of faulting

The character of the faults that deform the Bocharalla Qpg1 complex is typical of strike-slip faults. This interpretation is based on the following: (1) the faults are vertical and are markedly linear (Figs. 3 and 5); (2) the sense of vertical throw on the Ruices and Peñon faults changes along strike; (3) horizontal striations are present on a vertical fault surface of the Ruices fault; (4) two of the three faults that deform the Bocharalla Qpg1 complex and the Alcora Qpg1 complex seem to cause both extension and shortening at the same time (c.f. Sylvester, 1988). For example, the Peñon splay terminates in a zone of extensional structures (Fig. 3), but the Peñon fault at the eastern edge of the Alcora Qpg1 complex is an oblique vertical fault that has a strong component of Quaternary vertical throw suggestive of shortening. The small graben formed along the trace of the Ruices fault is entirely on the upthrown block (Figs. 3 and 12). Finally, the prominent fault scarp that denotes the Ruices fault trace on the Bocharalla Qpg1 complex suggests dip slip on a vertical fault resulting from shortening.

Quaternary deformation in the Bocharalla Qpg1 complex included left lateral oblique slip faulting. Although some of the structures indicating this type of slip are in Middle Miocene marl and fault breccia of unknown age, it can be concluded that left lateral oblique movements are Quaternary because: (1) the fault surfaces on which some striations were measured are in unconsolidated Miocene marl, but are unweathered and very well preserved; (2) the faults offset Quaternary deposits elsewhere along their traces; and (3) right lateral shear occurred in the Alpujarran Corridor through the Late Pliocene/Early Quaternary (Rodríguez Fernández et al., 1990). It is, therefore, unlikely that left lateral oblique slip occurred before the Pliocene, and because the faults deform Qpg1, left lateral oblique slip probably occurred since the Mid Pleistocene.

Mid to Late Quaternary faulting in the EAC provides an insight into the local strain field. Based on the attitude of fault surfaces, on the association of shortening and extensional features along the traces of faults and on striations indicating left lateral oblique slip, it is concluded that faults in the Bocharalla Qpg1 comprise a zone of minor left lateral shear. Dip slip on the faults is suggestive of shortening.

7.4. Deformation of Qpg1 landforms

East of Padules (Fig. 2), Qpg1 gravels and the smooth unconformities (straths and pediments) they overlie dip towards Río Andarax and away from Sierra de Gádor or Sierra Nevada mountain fronts (García, 2001). Given the locations of the Bocharalla fault trace, it can be concluded that the southward dip (toward the mountain front) of Qpg1 deposits and the unconformity they overlie at the distal western lobe was caused by south-side up faulting along the Bocharalla fault.

Interpretation of detailed field geomorphic mapping and observations show that the tread of the western lobe of the Bocharalla Qpg1 complex is also tilted. Surfaces of alluvial fans underlain by Qpg1 gravels throughout the EAC slope toward Río Andarax and away from Sierra de Gádor or Sierra Nevada mountain fronts (García, 2001). Streams that deposited Qpg1 alluvial fan gravels are incised below Qpg1 fan surfaces and flow perpendicular to and away from mountain front trends and drain directly into the modern Río Andarax. Younger streams developed on degraded Qpg1 surfaces flow perpendicular to and away from the local trend of the mountain front. Compared to other Qpg1 landforms in the EAC, the drainage pattern on the distal part of the western lobe of the Bocharalla Qpg1 complex is unusual (Fig. 3). Assuming that like other Qpg1 fan surfaces, the

western lobe surface sloped toward Río Andarax when the Qpg1 gravels that underlie it were deposited, then the drainage pattern developed on the NW corner of the western lobe indicates that its surface is tilted down to the south. This result is significant because it attests to relatively recent tectonism and supports interpretations regarding the timing of deformation based on correlation of Qpg1 to AdA travertine.

8. Discussion

In this section, the factors that controlled Mid Quaternary to present landscape evolution in the EAC are evaluated. A fundamental objective of this section is presenting a model for Mid Quaternary to recent landscape development in the EAC. Another objective is to propose a model for development of topographic relief in the Internal Zone of the Betic Cordillera during Quaternary time. The models are developed by assessing the relative roles of eustasy, climate and deformational style in the Quaternary landscape evolution history of the EAC. Also critical to this discussion is estimating rates of fluvial incision and rock uplift.

8.1. The role of eustasy in Quaternary evolution of the EAC fluvial system

The role of Quaternary eustatic fluctuation is negligible in the evolution of the EAC fluvial system (García, 2001). Flume studies showed that if a coastal area has a low gradient continental shelf, then base level lowering resulting from eustatic fluctuation causes progradation of a fan delta over the subaerial continental shelf (Schumm, 1993). Recent field studies also show that fluvial aggradation across an exposed continental shelf occurs during eustatic lows in localities where the shelf has a low gradient (e.g., Harvey et al., 1999; Pazzaglia and Brandon, 2001).

The Cabo de Gata area in southern Spain (Fig. 2) is one field example of the situation predicted in the flume experiments summarized in Schumm (1993). As a result of increased sediment delivery to streams and a relatively shallow shelf, coastal alluvial fans prograded over the shelf during the last glacial maximum/eustatic low (Harvey et al., 1999). Because of the shallow shelf off-shore of the Andarax rivermouth (SHOM, 1987; IHM, 1999) and because of the relatively large amount of sediment delivered to larger fluvial systems, it is likely that large streams in southern Spain, like the Río Andarax, do not incise appreciably during eustatic lows (Harvey et al., 1999, personal communication). This inference is supported by the absence of a well developed submarine canyon offshore of the present day Río Andarax mouth and delta (SHOM, 1987; IHM, 1999). In addition, tectonically induced stream incision in the middle reaches of major trunk streams is uninterrupted during eustatic rises and eustatic high stands (Merritts et al., 1994; Personius, 1995) and the EAC coincides with the middle reaches of the Río Andarax.

8.2. The role of climate in Quaternary landscape and fluvial system evolution in the EAC

The role of climatic fluctuation in EAC landscape evolution is minor compared to the role of tectonism. Fluvial aggradation during glacial maxima (e.g., Harvey, 1990) had a limited effect: vertical stream incision stopped in the EAC during ois8, but fluvial aggradation resulting from post-ois8 time glacial intervals stopped vertical incision only in the area upstream of Rambla de Juan de Campos (Fig. 2; García, 2001). Fluvial sediments younger than Qpg1 and AdA sequences are relatively rare in the EAC downstream of Rambla de Juan de Campos. This indicates that streams downstream of and including Rambla de Juan de Campos (Figs. 2–4) have been downcutting continuously since ois8 (García, 2001). Downcutting results from a tectonically induced "incision wave" that is moving through the Andarax fluvial network (García, 2001; see discussion below). Climatic fluctuations have not caused aggradation downstream of Rambla de Juan de Campos (Fig. 2) since ois8 because of the incision wave and because of limited sediment availability (c.f., Harvey et al., 1999; García, 2001).

8.3. Quaternary faulting in the EAC

Post-ois8 time, left lateral slip on faults in the Alpujarran Corridor is noteworthy in light of models proposed for eastern Betic Cordillera Quaternary tectonism. The models postulate collision between

Africa and Europe at the Iberian Peninsula is accommodated by a crustal scale, left lateral shear zone that extends from Alicante in the NE to Cabo de Gata in the SW (Fig. 1; "Trans-Alboran shear zone" of De Larouzière et al., 1988). We speculate that left lateral shear related to accommodation of African–Iberian convergence along the Trans-Alboran shear zone is affecting areas as far northwest as the Alpujarran Corridor, which is approximately 50 km northwest of Cabo de Gata (Fig. 1). The component of dip slip on the faults is attributed to the Quaternary and present day regional stress field in the Internal Zone of the Betic Cordillera ($\sigma 1$ horizontal and oriented N–S to NNW–SSE; e. g., Galindo-Zaldívar et al., 1993).

The character of the Bocharalla complex faults (typical of strike-slip faults) can be explained in two ways. One possibility is that the faults are fundamentally strike-slip faults that formed to accommodate left lateral shear transferred from the Trans-Alboran shear zone. In this model, N–S compressional stress is not as prevalent as left lateral shear and is manifest as the vertical component of oblique slip. Another possibility is that as elsewhere in the western part of the Internal Zone, Quaternary deformation in the Bocharalla Qpg1 complex is accommodated by faults formed in the Miocene Epoch (Sanz de Galdeano, 1990). In this model, the character of Bocharalla complex faults reflects their development as vertical, right lateral strike-slip faults during Miocene tectonism (Sanz de Galdeano, 1996). When Mid and Late Quaternary stresses acted on them, they propagated into Quaternary sediments as vertical faults. If this is the case, it cannot be determined whether left lateral shear or N–S compressional stress is prevalent.

8.4. Stream incision and rates of regional rock uplift since ois8

Analyses of faulting provides insight regarding Mid and Late Quaternary stresses in the EAC, but faulting was localized, relatively small magnitude and did not significantly affect long-term landscape development. This paper shows that the maximum vertical displacement along Quaternary faults is about 10 m and that eustasy had a negligible impact on the EAC fluvial system. The deeply incised fluvial network of the EAC, which includes streams entrenched 100 m or more in subvertical gorges, attests to recent, tectonically driven base-level lowering (García, 2001; c.f., Pazzaglia et al., 1998). The lack of significant faulting within the EAC indicates that the type of deformation driving stream incision is regional uplift of the entire EAC (García, 2001).

Large bedrock streams or streams with mixed alluvial/bedrock channels in tectonically active areas typically incise at a rate within 70% of the regional rock-uplift rate (Pazzaglia et al., 1998). Under certain conditions streams in tectonically active areas incise at a rate equal to the rate of rock uplift (Merritts et al., 1994; Personius, 1995; Pazzaglia et al., 1998; Pazzaglia and Brandon, 2001). Bedrock streams or streams with mixed alluvial/bedrock channels incising at a rate equal to rock uplift rate are analogous to "graded" alluvial streams and are said to be in "steady state" (Pazzaglia et al., 1998). Given the relatively large catchment area of Río Andarax (1270 km^2 in the EAC; 2027 km^2 total) and the high erodibility of the material it flows through downstream of Padules, it is likely that between Padules and Alhama de Almería, the Río Andarax can incise at a rate equal to the rock uplift rate in the EAC (c.f., Merritts et al., 1994; Pazzaglia et al., 1998).

Relatively slow Río Andarax incision rates upstream of Padules (Fig. 2 and Table 3) are readily reconciled within a framework of the EAC's geomorphic history. The Río Andarax drainage network downstream of, and including Barranco del Bosque (the Padules/Almócita Qpg1 feeder stream; Fig. 2), was affected by an incision wave prior to ois8 (García, 2001). The incision wave did not reach Los Llanillos de Cacín until after ois8 (Fig. 2; García, 2001). A knickpoint is present in Río Andarax's channel less than 1 km upstream of Barranco del Bosque (Fig. 8). The convex-up morphology of the reach upstream of the knickpoint suggests that it is not at steady state because the incision wave is still passing through it (c.f. Safran, 1998; García, 2001). Downstream of the knickpoint, the Río Andarax channel is smooth and is slightly concave up, which suggests that it is in steady state (c.f. Pazzaglia et al., 1998).

Useful comparisons can be made between the Rio Andarax and the Río Jemez in New Mexico, USA. Río Jemez is in steady state and is incising at the same rate as regional rock uplift (Pazzaglia et al., 1998). This is significant because like Río Andarax, Río

Jemez has a mixed bedrock/alluvial channel (Pazzaglia et al., 1998; García, 2001) and these rivers are similar in many other ways. The longitudinal profile of Río Andarax downstream of Padules is similar to the longitudinal profile of Río Jemez in the reach that is incising at a rate equal to rock uplift rate. Both rivers are in semiarid climatic settings (30–50 mm annual precipitation) and both rivers flow over weak substrate. Their catchment areas are also similar (Río Jemez: 1200 km^2 in the studied reach, 2700 km^2 total; Pazzaglia et al., 1998). Based on the shape of Río Andarax's longitudinal profile downstream of Padules and on its similarity to the shape of Río Jemez's longitudinal profile, it can be concluded that Río Andarax is in steady state downstream of Padules in the EAC, where it is incising at a rate equal to rock uplift rate.

Differences in the Río Andarax incision rate downstream of Padules can result from two factors. The rates may vary because the data used to determine incision rates are the bases of tributary landforms whose toes are cut back by erosion. The deposits that underlie the landforms dip towards Río Andarax and, therefore, the bases of landforms that are more eroded are higher above the Río Andarax channel. Alternatively, the variation may be due to along-channel changes in uplift rate (e.g., Pazzaglia et al., 1998). The available data cannot be used to distinguish between these two factors. Therefore, the incision rates which best approximate ois8 to present rock uplift rates for the EAC can be only be constrained to between 0.3 and 0.7 m/ka (Table 2). These are maximum rates, because they are determined from piedmont deposits whose toes are cut back by varying amounts.

The calculated rates are comparable to rates for 500 ka to present uplift of Sierra Nevada's western flank relative to the adjacent Padul basin (0.42–0.84 m/ka; Sanz de Galdeano and López Garrido, 1999; Fig. 1). The rates are also comparable to, but slightly greater than, long-term uplift rates determined from the elevation of Tortonian marine deposits on Sierra de Gádor. The deposits are 8 km south of Rágol (Fig. 2) and are at an altitude of 1600 m (IGME, 1980; Martín, 1999, personal communication). Their present elevation requires uplift rates ranging from 0.17 m/ka (since middle Tortonian time) to 0.23 m/ka (since latest Tortonian time).

8.5. The role of tectonism in Quaternary topographic development of the eastern Alpujarran Corridor

Differential erosion of rocks juxtaposed along EAC border faults played a fundamental role in development of topographic relief between the EAC and adjacent uplands. For example, the Sierra de Gádor mountain front between Alicún and Rágol (Figs. 2 and 7) is a 500–600-m high escarpment that is linear at a scale of a few kilometers. Features indicative of fault-controlled mountain front morphology, like triangular facets, are not present on this or any other mountain fronts adjacent to the EAC (Figs. 7 and 9). Linear escarpments in semiarid climates commonly form by erosional exhumation of older, inactive structures (e.g., Formento-Trigilio and Pazzaglia, 1998). Accordingly, the most plausible explanation for how the dramatic escarpment west of Alhama de Almería formed is erosional exhumation of a paleo basin-bounding fault.

Exhumation of paleostructures in semiarid settings is facilitated by the variable erodibility of juxtaposed rocks, but is driven by fluvial erosion related to regional uplift (Formento-Trigilio and Pazzaglia, 1998). The onset of regional uplift and stream incision in the EAC is estimated on the basis of previous studies (Goy and Zazo, 1986; Pascual Molina, 1997; García, 2001). Upper Pliocene/Lower Pleistocene PQc gravels were deposited on the hanging wall of a NW–SE striking, NE dipping normal fault that intersects the northeastern corner of the EAC (Pascual Molina, 1997). Straths and pediments carved into PQc and overlain by AdA travertine sequences indicate that by ois8, the former hanging wall of the fault that controlled the deposition of PQc (Pascual Molina, 1997) was subject to regional uplift that affected the rest of the EAC. Ongoing tectonism along the southern mountain front of Sierra de Gádor began in the earliest Middle Pleistocene (Goy and Zazo, 1986), which is from 780 to 200 ka (Berggren et al., 1995). Deformation includes regional tilting in Campo de Dalías (Goy and Zazo, 1986), which is 20–25 km southeast of the EAC (Fig. 1). The morphostratigraphy of Qpg1 indicates that by the beginning of ois8, streams in the EAC east of Padules were incising in response to regional uplift (García, 2001). Therefore, on the basis of the data of Goy and Zazo (1986) and García (2001), the best estimate for onset of ongoing,

regional uplift in the EAC is up to a few hundred thousand years before ois8 and as early as the earliest Middle Pleistocene.

Assuming the Río Andarax incision rate from 750 ka to ois8 was the same as it was from ois8 to recent times, incision by the Río Andarax can account for 225 to 525 m of base-level lowering at the Sierra de Gádor mountain front between Alicún and Rágol. This suggests that fluvial incision driven by regional uplift can account for between 40% and 90% of the topographic relief along the steepest and highest part of the northern Sierra de Gádor mountain front. Topographic relief between the ois8 paleofluvial level and modern valley bottoms also results from stream incision caused by regional uplift (García, 2001). Therefore, it is likely that the relief between the EAC and adjacent mountain ranges is largely a result of fluvial erosion. Stream incision driven by regional uplift is the primary factor controlling formation of the eastern Alpujarran Corridor topographic depression. Pre-Quaternary dip slip on EAC border faults may have played a role, but that role was secondary to fluvial denudation.

8.6. Implications for regional tectonics and topography

The most noteworthy aspects of Quaternary deformation in the Alpujarran Corridor are the absence of significant faulting and the prevalence of regional uplift. It is also noteworthy that topographic relief between Internal Zone bedrock massifs and the EAC results primarily from fluvial denudation driven by regional uplift. Based on these insights and on previous studies, a model is proposed relating African–Iberian convergence and topographic development in the Internal Zone of the Betic Cordillera.

Neogene and Quaternary extensional uplift along Sierra Nevada's western and southwestern flanks is related to a NNE striking, oblique normal/left lateral, crustal-scale fault or fault zone (Fig. 1; Sanz de Galdeano and López Garrido, 1999). This structure accommodates E–W extension resulting from N–S shortening (Sanz de Galdeano and López Garrido, 1999). The high point of Sierra Nevada's crest is Mulhacén peak (altitude 3479 m). Mulhacén is at the western end of the crest and about 10 km east of the crustal scale, NNE striking fault zone of Sanz de Galdeano and López Garrido (1999). The elevation of Sierra Nevada's crest decreases to the east and its easternmost high peak is Montenegro (altitude 1711 m; Montenegro is about 7 km NNW of Rágol; Figs. 1 and 2). Thus, Sierra Nevada's fault-bounded, 2.5-km high western front culminates in a 55-km long, gently eastward sloping topographic crest. This morphology suggests a large scale, tilted and uplifted footwall block of a normal fault. We propose that the EAC is in the uplifted footwall of a large structural block that includes Sierra Nevada and the Alpujarran Corridor (Figs. 1 and 2). In the context of this model, fluvial denudation in the EAC is driven by regional uplift, as well as uplift of the Sierra Nevada/Alpujarran Corridor footwall block. Minor left lateral slip on E–W striking faults in the EAC indicate that the eastern end of the Sierra Nevada/Alpujarran Corridor tilted footwall block is subject to stresses arising from shear along the ENE striking Trans Alboran crustal scale fault system. However, faulting arising from these stresses played a negligible role in the Quaternary topographic development of the EAC.

On the basis of this model of recent topographic and structural evolution in the Sierra Nevada/Alpujarran Corridor area, a notion emerges of how faulting, topography and regional uplift in the Internal Zone of the Betic Cordillera are related to Quaternary shortening caused by collision of the African and European plates. Regional uplift, probably caused by crustal-scale underthrusting of the Iberian Peninsula margin beneath the Internal Zone of the Betic Cordillera (Galindo-Zaldívar et al., 1997), was documented in the Malaga Basin (Sanz de Galdeano and López-Garrido, 1991), the Granada Basin (Sanz de Galdeano and López Garrido, 1999), the Guadix Basin (Viseras and Fernández, 1992), the eastern Alpujarran Corridor (this paper), the Sorbas Basin (e.g., Mather, 2000) and the Vera Basin (Stokes and Mather, 2000; (Fig. 1). Significant Quaternary faulting has been documented locally in the Internal Zone of the Betic Cordillera and two crustal-scale fault zones have been active in the Quaternary, but the only Quaternary deformational style common to the entire Internal Zone is regional uplift. During the Quaternary, development of topographic relief within the Internal Zone due to faulting is restricted to areas within a few kilometers to a few tens of kilometers of crustal-scale fault zones. Farther away from crustal scale fault zones, topographic relief between Internal Zone bedrock massifs and surround-

ing exhumed Neogene basins formed as a result of fluvial denudation driven by regional uplift.

9. Conclusions

Calcrete-cemented gravel (Qpg1) together with interbedded travertine and clastic sediments (AdA sequences) denote an oxygen isotope Stage 8 (ois8; 303–245 ka; Imbrie et al., 1984) paleofluvial level in the eastern Alpujarran Corridor (EAC). Qpg1 deposits are locally faulted and tilted. The character of faults in Qpg1 indicate that deformation is caused by left lateral shear associated with the nearby Trans-Alboran shear zone of De Larouzière et al. (1988). Faulting is also related to regional N–S to NNW–SSE compression in the Internal Zone of the Betic Cordillera.

A range of maximum incision rates since 245 ka is calculated for the Río Andarax (the EAC axial stream) from the height of the ois8-time paleofluvial level above the present-day Andarax channel. These Río Andarax incision rates are equal to regional rock-uplift rates in the EAC and are between 0.3 and 0.7 m/ka. Eustasy, climate and faulting had negligible roles in Quaternary topographic development of the EAC. Most of the topographic relief between the EAC topographic trough and surrounding mountain ranges formed as a result of fluvial incision driven by regional uplift.

A model is proposed relating Quaternary tectonism and topographic development in the Internal Zone of the Betic Cordillera. Regional uplift affected all of the Internal Zone, but within the Internal Zone, uplift of mountain ranges caused by faulting only occurred near crustal-scale structures. In the Mid to Late Quaternary Period, topographic relief between Internal Zone bedrock massifs and surrounding basins formed largely as a result of fluvial denudation driven by regional uplift.

Acknowledgements

This paper benefited greatly from review and comments by F.J. Pazzaglia, M. Stokes, A.G. Sylvester and an anonymous reviewer. The first author would like to thank the following people for generous support and/or assistance while conducting field work: the Valdivia López family, Dr. Alice Alldredge and James M. King, Enrique Pérez Ibarra (a friend of the first author), Petra, Dr. A. Azor, Dr. R. El Hamdouni, Dr. C. Irigaray Fernández, Dr. K. Kleverlaan and, especially, Drs. A.E. Mather and M. Stokes. Enrique Pérez Ibarra located travertine sample T-12 and directed the first author to critical travertine sampling sites.

This research was funded by the following organizations and grants: Vicerrectorado de investigación y relaciones internacionales, Facultad de Ciencias, University of Granada, Spain; Geological Society of America Research Grant; Sigma Xi Grant-in-aid of Research; University of California, Santa Barbara (UCSB) Academic Senate; UCSB Department of Geological Sciences "Block Grants."

References

Alonso-Zarza, A.M., Silva, P.G., Goy, J.L., Zazo, C., 1998. Fan-surface dynamics and biogenic calcrete development: interactions during ultimate phases of fan evolution in the semiarid SE Spain (Murcia). Geomorphology 24, 147–167.

Berggren, W.A., Kent, D.V., Swisher III, C.C., Aubry, M.P., 1995. A revised Cenozoic geochronology and chronostratigraphy. In: Berggren, W.A., Kent, D.V., Aubry, M.-P. (Eds.), Geochronology, Time Scales and Global Stratigraphic Correlation. Society of Economic Paleontologists and Mineralogists Special Publication, vol. 54. SEPM, Tulsa, pp. 129–212.

Bull, W.B., 1990. Stream-terrace genesis: implications for soil development. Geomorphology 3, 351–367.

Crombie, M.K., Arvidson, R.E., Sturchio, N.C., El Alfy, Z., Abu Zeid, K., 1997. Age and isotopic constraints on Pleistocene pluvial episodes in the Western Desert, Egypt. Palaeogeography, Palaeoclimatology, Palaeoecology 130, 337–355.

De Larouzière, F.D., Bolze, J., Bordet, P., Hernandez, J., Montenat, C., Ott d'Estevou, P., 1988. The Betic segment of the lithospheric Trans-Alboran shear zone during the Late Miocene. Tectonophysics 152, 41–52.

Formento-Trigilio, M.L., Pazzaglia, F.J., 1998. Tectonic geomorphology of the Sierra Nacimiento: traditional and new techniques in assessing long-term landscape evolution in the southern Rocky Mountains. The Journal of Geology 106, 433–453.

Galindo-Zaldívar, J., González-Lodeiro, F., Jabaloy, A., 1993. Stress and paleostress in the Betic–Rif Cordilleras. Tectonophysics 227, 105–126.

Galindo-Zaldívar, J., Jabaloy, A., González-Lodeiro, F., Aldaya, F., 1997. Crustal structure of the central Betic Cordillera (SE Spain). Tectonics 16, 18–37.

García, A.F., 2001. Quaternary stream incision and topographic development in the eastern Alpujarran Corridor, Betic Cordillera, southern Spain (Almería). PhD thesis, The University of California, Santa Barbara, USA, 214 pp.

Goy, J.L., Zazo, C., 1986. Synthesis of the Quaternary in the Almería Littoral neotectonic activity and its morphologic features, western Betics, Spain. Tectonophysics 130, 259–270.

Harvey, A.M., 1990. Factors influencing Quaternary alluvial fan development in southeast Spain. In: Rachocki, A.H., Church, M. (Eds.), Alluvial Fans: A Field Approach. Wiley, Chichester, pp. 247–269.

Harvey, A.M., Silva, P.G., Mather, A.E., Goy, J.L., Stokes, M., Zazo, C., 1999. The impact of Quaternary sea-level and climate change on coastal alluvial fans in the Cabo de Gata ranges, southeast Spain. Geomorphology 28, 1–22.

IGME, 1980. Mapa Geologico Almería-Garrucha 84–85. Instituto Geologico y Minero de España, 1:200,000 scale.

IHM, 1999. Puerto de Almeria. Carta de la serie Internacional, mar Mediterranea, Costa sur de España. Instituto Hidrografico de la Marina, Cadiz, España, 1:10,000 scale.

Imbrie, J., Hays, J.D., Martinson, D.G., McIntyre, A., Mix, A.C., Morley, J.J., Pisias, N.G., Prell, W.L., Shackleton, N.J., 1984. The orbital theory of Pleistocene climate: support from a revised chronology of the marine $\delta^{18}O$ record. In: Berger, A., Imbrie, J., Hays, J., Kukla, G., Saltzman, B. (Eds.), Milankovitch and Climate. D. Reidel Publ. Co., Dordrecht, pp. 269–305. Part 1.

Machette, M.N., 1985. Calcic soils of the southwestern United States. In: Weide, D.L. (Ed.), Soils and Quaternary Geology of the Southwestern United States. Geological Society of America Special Paper, vol. 203. Geol. Soc. Am., Denver, pp. 1–21.

Mather, A.E., 2000. Impact of headwater river capture on alluvial system development: an example from the Plio-Pleistocene of the Sorbas Basin, SE Spain. Journal of the Geological Society of London 157, 957–966.

Merritts, D.J., Vincent, K.R., Wohl, E.E., 1994. Long river profiles, tectonism, and eustasy: a guide to interpreting fluvial terraces. Journal of Geophysical Research 99 (B7), 14031–14050.

Nash, D.J., Smith, R.F., 1998. Multiple calcrete profiles in the Tabernas Basin, southeast Spain: their origins and geomorphic implications. Earth Surface Processes and Landforms 23, 1009–1029.

Pascual Molina, A.M., 1997. La Cuenca Neogena de Tabernas (Cordilleras Beticas). PhD thesis, University of Granada, Granada, Spain.

Pazzaglia, F.J., Brandon, M.T., 2001. A fluvial record of long-term steady-state uplift and erosion across the Cascadia forearc high, western Washington State. American Journal of Science 301, 385–481.

Pazzaglia, F.J., Gardner, T.W., Merritts, D.J., 1998. Bedrock fluvial incision and longitudinal profile development over geologic time scales determined by fluvial terraces. In: Tinkler, K.J., Wohl, E.E. (Eds.), Rivers Over Rock, Geophysical Monograph, vol. 107. The American Geophysical Union, Washington, DC, pp. 207–235.

Personius, S.F., 1995. Late Quaternary stream incision and uplift in the in the forearc of the Cascadia subduction zone, western Oregon. Journal of Geophysical Research 100 (B10), 20193–20210.

Rodríguez Fernández, J., Sanz de Galdeano, C., Vera, J.A., 1990. Le Couloir des Alpujarras. In: Montenat, C. (Ed.), Les Bassins neogenes du domaine Betique oriental (Espagne), tectonique et sedimentation dans un couloir de decrochement: I. Etude regionale, Paris, Institut: Geologique Albert de Lapparent, 1990. Documents et Travaux de l'Institut Geologique Albert de Lapparent, 0248-9589, vols. 12–13. L'Institut Geologique Albert de Lapparent, Paris, pp. 87–100.

Safran, E.B., 1998. Channel network incision and patterns of mountain geomorphology. PhD thesis, The University of California, Santa Barbara, USA.

Sanz de Galdeano, C., 1990. Geologic evolution of the Betic Cordilleras in the Western Mediterranean, Miocene to present. Tectonophysics 172, 107–119.

Sanz de Galdeano, C., 1996. The E–W segments of the contact between the External and Internal Zones of the Betic and Rif Cordilleras and the E–W corridors of the Internal Zone (a combined explanation). Estudios Geologicos 52, 123–136.

Sanz de Galdeano, C., 1997. La Zona Interna Bético–Rifeña. Monográfica Tierras del Sur, vol. 18. Editorial Universidad de Granada, Univ. of Granada, Spain.

Sanz de Galdeano, C., López-Garrido, A.C., 1991. Tectonic evolution of the Malaga Basin (Betic Cordillera). Regional implications. Geodinamica Acta 5, 173–186.

Sanz de Galdeano, C., López Garrido, A.C., 1999. Nature and impact of the Neotectonic deformation in the western Sierra Nevada (Spain). Geomorphology 30, 259–272.

Sanz de Galdeano, C., Vera, J.A., 1992. Stratigraphic record and paleogeographical context of Neogene basins in the Betic Cordillera, Spain. Basin Research 4, 21–36.

Sanz de Galdeano, C., Rodriguez-Fernandez, J., Lopez-Garrido, A.C., 1986. Tectonosedimentary evolution of the Alpujarran corridor (Betic Cordillera, Spain). Giornale di Geologia 48/1–2, 85–90.

Sanz de Galdeano, C., Rodríguez Fernández, J., López Garrido, A.C., 1991. Geologic map of the Alpujarran Corridor. Deposito Legal GR-830-1991, printed by T.G. Arte, Juberias and CIA, S.A., Marracena (Granada), España. 1:50,000 scale.

Schumm, S.A., 1993. River response to baselevel change: implications for sequence stratigraphy. The Journal of Geology 101, 279–294.

SHOM, 1987. Carte Spéciale 'S' de la Pointe del Sabinal a Carthagène 4718 S. Service Hydrographique et Océanographique de la Marine, Brest Cedex, France, 1:247,000 scale.

Stokes, M., Mather, A.E., 2000. Response of Plio-Pleistocene alluvial systems to tectonically induced base-level changes, Vera Basin, SE Spain. Journal of the Geological Society of London 157, 303–316.

Sylvester, A.G., 1988. Strike-slip faults. Geological Society of America Bulletin 100, 1666–1703.

Viseras, C., Fernández, J., 1992. Sedimentary basin destruction inferred from the evolution of drainage systems in the Betic Cordillera, southern Spain. Journal of the Geological Society of London 149, 1021–1029.

Williams, D.F., Thunnel, R.C., Tappa, E., Rio, D., Raffi, I., 1988. Chronology of the Pleistocene oxygen isotope record: 0–1.8 m.y. B.P. Paleogeography, Paleoclimateology, Paleoecology 64, 221–240.

Wright, V.P., Tucker, M.E., 1991. Calcretes: an introduction. In: Wright, V.P., Tucker, M.E. (Eds.), CalcretesInternational Association of Sedimentologists, Reprint Series, vol. 2. Blackwell, Oxford, UK, pp. 1–22.